Aerosol-based techniques for distinguishing ion from nano toxicity

Angeliki Kourmouli

B.Sc. Thesis

Supervisors:

Assist. Prof. Dr. George Biskos

Assist. Prof. Dr. Olga-Ioanna Kalantzi

Mytilene, 2013

Acknowledgements

To my family...

Abstract

The increasing penetration of products containing engineered nanoparticles (ENPs) has raised many concerns with respect to their environmental impacts (Scown et al, 2010). Due to the high variability of ENPs (i.e., in size, morphology, and composition), determining their impacts requires standardized methods for measuring potential nanoparticle spills in the environment, as well as techniques for assessing their toxicity on living cells. With respect to the latter, to date there is lack of universal technique for assessing nanoparticle toxicity (Oberdörster, 2005). This is reflected by the vast number of works which in many cases report measurements that are contradicting one another (cf. Hamouda et al, 2000; Sondi and Salopek-Sondi, 2004).

In this thesis I demonstrate the use of aerosol-based techniques for assessing the toxicity of ENPs on living cells. Compared to wet-chemistry techniques, generating test nanoparticles by aerosol-based methods has the advantage of higher purity, as well as of better control over their size, morphology and composition. For the experiments described here I generated Ag and Au nanoparticles (NPs) by two aerosol-based methods; the first one employed a tube furnace whereas the second one a spark discharge. These two techniques produced aerosols containing particles of different sizes and in different concentrations.

The method employed to assess the toxicity of the NPs is the one that is used to assess the susceptibility of microorganisms in antibiotics. Although no apparent trends with respect to particles size are observed, whereas with respect to the particles concentrations in the preliminary experiments there was a small increase as the concentration increased and at the subsequent experiments no trends were observed; my results clearly demonstrate that this method can be employed to distinguish between ion and nano toxicity of ENPs.

Table of contents

1. Introduction

'*Why cannot we write the entire 24 volumes of the Encyclopaedia Brittanica on the head of a pin?*' Richard P. Feynman, an American Physicist, wondered at his speech titled "There's Plenty of Room at the Bottom" on the 29th of December 1959, at the annual meeting of the American Physical Society at the California Institute of Technology. By this question Dr. R. Feynman indicated the greater range of possible properties that substances can have if some control can be succeeded in the arrangement of things on a small scale (Zyvex, n.d.). Many scientists believe that this speech was the birth of a new field, the field of Nanoscience. Nanoscience refers to the science for the understanding of chemical and biological structures with dimensions in the range from 1-100 nanometers. At this scale, properties like electrical, mechanical, optical, chemical and biological differ to a great extent from molecular properties. The application of this science is called Nanotechnology. Nanotechnology is the ability to manipulate and work at the molecular level, atom by atom, to create large structures with fundamentally new molecular organization. The aim of this technology is to exploit these novelties by gaining control of structures and devices at atomic, molecular, and supramolecular levels and to learn to efficiently manufacture and use these devices (US National Science and Technology Council, 2000). It's contribution will be determinant to other science and technology obstacles; for example, in health (advanced drug delivery and targeting capabilities), in industry (improved printing and lasers), in environment (advanced chemicals and bio-detectors), etc (Mansoori, 2005).

A nanometer is one billionth of a meter, i.e, 10^{-9} m. The prefix 'nano', comes from the Greek word 'nanos' (νάνος) which stands for 'dwarf'. The nanometer scale is very important because the physic-chemical properties of materials with nanosized dimensions may vary from those of the bulk materials due to quantum mechanical effects. For example, with the nanoscale a high surface-to-volume ratio the material can behave differently (Mansoori, 2005).

Nanomaterials are materials which have structured components (nanostructures) with at least one dimension less than 100nm. Depending on how many dimensions they have in the nanoscale, nanomaterials can be classified as:

- thin films, layers and surfaces, materials that have one dimension in the nanoscale,
- nanowires, nanotubes and biopolymers, materials that have two dimensions in the nanoscale,
- nanoparticles, fullerenes, dendrimers, quantum dots and nanocrystalline materials, materials that have three dimensions in the nanoscale.

Nanomedicine is the diagnose, treatment, and prevention of disease and traumatic injury, and preservation and improvement of human health, are achieved with the use of molecular tools and molecular knowledge of the human body (Freitas, 2005).

Quantum dots can detect the presence of many viruses in a blood sample at the same time. Furthermore, quantum dots are being investigated as chemical sensors, for cancer cell detection, gene mapping, genotyping, vascular imaging and many other applications. Additionally, soluble derivatives of fullerenes have good biocompatibility and low toxicity even at relatively high doses and can be used as antiviral and antibacterial agents. Nanomaterials, in general, are being investigated for a wide range of applications in cancer detection and treatment and many other serious and up until now untreatable diseases (Freitas, 2005).

The term nanoparticle is used to describe a sub-classification of ultrafine particle with lengths in two or three dimensions greater than 1 nm and smaller than about 100 nm. The nanoparticles' properties are related to their size, shape and composition (Mansoori, 2005). Nanoparticles in the environment are not only produced by human activities, but also by natural processes, such as volcanic eruptions, forest fires and photochemical reactions (Buzea, et al., 2007). Except from nanoparticles, other classifications are nanofibers and nanotubes. Nanofibers are fibers whose diameter is in the nanoscale range and nanotubes are nanoscaled tube structures.

As mentioned before, nanoparticles are produced from both natural processes and human activities and so they interact with ecosystems and living organisms. Regarding natural processes, do not pose threats to human health because most of these processes' products are soluble particles. Moreover, man-made particles can be either manufactured or produced by activities such as fossil fuel burning, diesel and engine exhausts, cigarette smoke, indoor pollution and building demolitions (Buzea et al, 2007).

A human is exposed to nanoparticles since there are in everyday products such as cosmetics, detergent, soaps, shampoos, liquid condoms, electrical and electronic parts. Furthermore, nanoparticles are also found in food colorants, fabrics, batteries, paints, plastics and anti-perspirants. The health effects are numerous and dependent on dose and entrypathways into the human organism (Buzea et al., 2007).

Possible pathways that particles can enter the human organism are through skin, inhalation, ingestion and genitals (Figure 1). Depending on the pathway, particles will end up in different organs and tissues, affect their functions and cause damages to the cells.
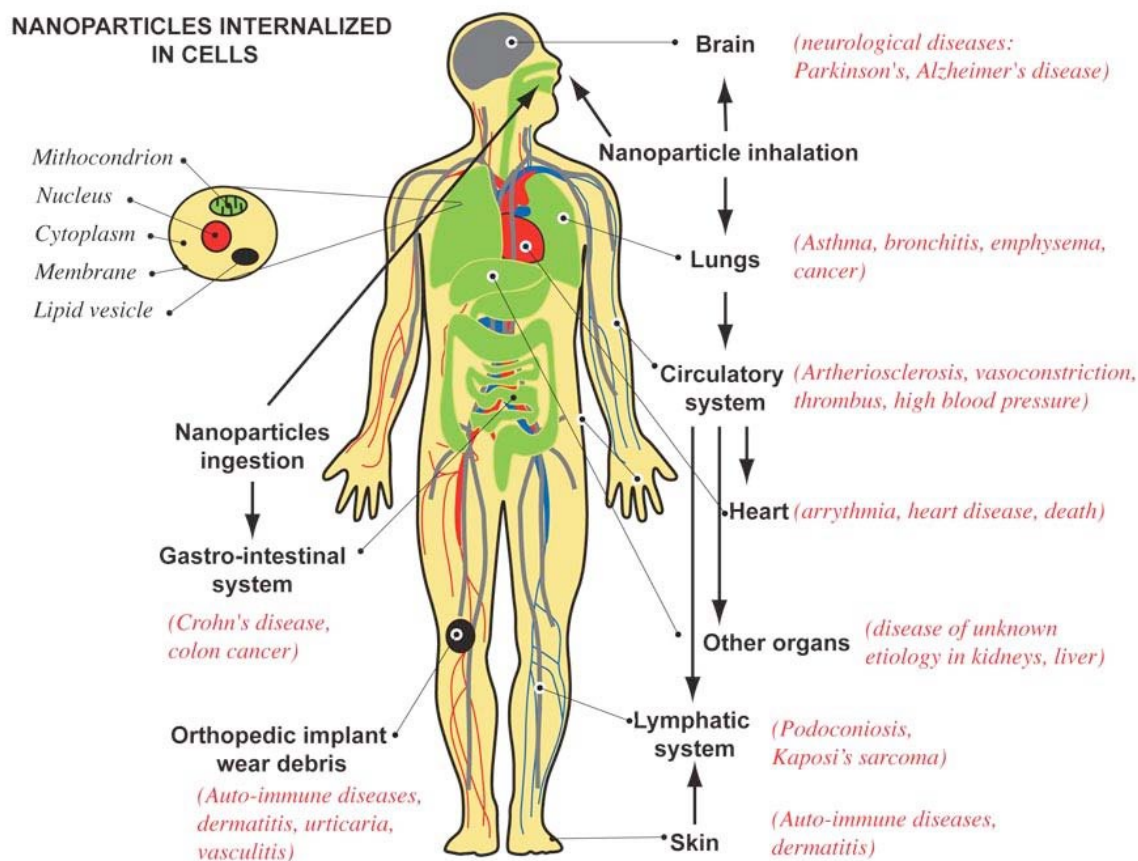
Figure 1: Schematics of human body with pathways of exposure to nanoparticles, affected organs, and associated diseases from epidemiological, in vivo and in vitro studies (Buzea, et al., 2007).

With this "intrusion" of nanoparticles in our lives it is necessary to be able to assess their toxic or harmful effects, before they penetrate the market and subsequently the ecosystems. Nanoparticles can end up in soil and affect bacteria important for farming and also, in the waste water endangering important aquatic organisms (Wijnhoven et al., 2009). Their effects on both biota and abiotic environment are yet unknown and their mechanism of action against cells and living organisms are based on assumptions because it is not fully understood. So, it is important to know if nanoparticles retain their unique properties after disposal to the environment, and at what level they may affect biological activity. Thus, a new field in Toxicology, which will investigate the effects of nanoparticles in human health is essential (Buzea et al., 2007). This is called Nanotoxicology.

The aim of this thesis is to investigate the toxic effects of engineered silver and gold nanoparticles produced with two different aerosol-based methods (i.e., the spark discharge and the vaporisation-condensation technique as described above) on the Gram-negative bacteria *Escherichia coli*. Moreover, another goal is to demonstrate any association between toxic effects with the size and the concentration of the nanoparticles. Another purpose is to investigate if the Kirby-Bauer disk diffusion method is capable of differentiating between ion- and nano-toxicity. Compared to wet-chemistry techniques, generating nanoparticles by aerosol-based methods has the advantage of higher purity, as well as of better control over their size, morphology and composition.

2. Literature review

The first part of this section describes the different techniques to produce NPs. The second part of this section provides information about the tested cells and a review of the existing literature on toxicity tests of ENPs, so that comparisons can be drawn between published research and this study.

2.1. Synthesis of ENPs and preparation of samples for toxicity tests

Except from the two aerosol-based techniques (vaporization-condensation technique and spark discharge technique), that will be discussed in later chapter, some techniques with which NPs can be produced will be cited.

One gas-phase technique is the Flame Spray Pyrolisis. One or more solid or liquid precursors along with organic solvents are placed into a stirred tank reactor (Wegner et al., 2011). In this reactor, dissolution and/or chemical conversion and mixing of the materials occur. With a pump the precursor solution goes to a spray nozzle and there it is atomized with oxygen (O_2) dispersion gas. Gases, among them O_2 and gaseous fuel for spray ignition and stabilization are moving to flame spray pyrolysis reactor through cylinders. Filtered ambient air is used to dilute and quench the hot flame aerosol before it enters the collection device, where NPs are gathered.

In a wet-chemistry technique silver seeds are formed by injection of $NaBH_4$ into an aqueous solution that contains $AgNO_3$ and sodium citrate (Pal et al., 2007). The solution is stirred and left for few hours to age. Then an aqueous solution of $AgNO_3$ is brought to boiling. An amount of the silver seeds solution and an aqueous solution of sodium citrate are added to the boiling solution. After the solution cools the AgNPs are purified by centrifugation.

Also, there NPs can be produced through bacteria and plants. Strains of *Streptococcus mutans* are inoculated on Muller-Hinton broth and left for 24 h incubation at 37 ºC (Nanda and Saravanan, 2009). Then the culture is centrifuged and the supernatant is added to a reaction vessel that contains $AgNO_3$. The reaction between Ag^+ and the supernatant is taking place in bright conditions. Bioreduction of Ag^+ occurs and AgNPs are produced.

2.2 Toxicity of ENPS

2.2.1 Description of bacteria

The Gram-negative bacteria *Escherichia coli* (*E.coli*) live in the human and animal intestines and are quite important for the proper function of the digestive tract. However, some strains are pathogenic and can cause infections, diarrhea, vomiting or fever. These infections are quite common, and can be transmitted through contact with other people or animals and contaminated water or food (Center for Disease Control and Infection, n.d.).

The terms 'Gram-negative' and 'Gram-positive' is used for differentiation among bacteria according to the Gram stain test. In this test, a purple crystal violet dye is used to make the bacteria cell wall visible under the microscope.. Gram-positive bacteria retain a purple color whereas Gram-negative a pink/red color (National Institute of Allergy and Infectious Diseases, n.d.). This difference in the stain color is due to the structure of the bacterial cell envelope.

While Gram-negative and Gram-positive bacteria have similar internal structure, they differ significantly in the external structure. Gram-negative bacterial cell wall is more intricate in both structure and chemistry than Gram-positive bacterial wall. Gram-positive bacteria have a thick multilayered cell wall that surrounds the cytoplasmic membrane, consisting mainly of peptidoglycan. The cell wall of Gram-positive bacteria contains teichoic acids, a type of bacterial polysaccharides which are absent from the Gram-negative bacteria. In contrast, Gram-negative bacterial cell wall is composed of a single layer of peptidoglycan surrounded by a membranous structure called the outer membrane, which contains lipopolysaccharides . Because of the thin peptidoglycan layer, Gram-negative bacteria cannot retain the violet stain during the Gram stain test (Medical Microbiology, 2002).
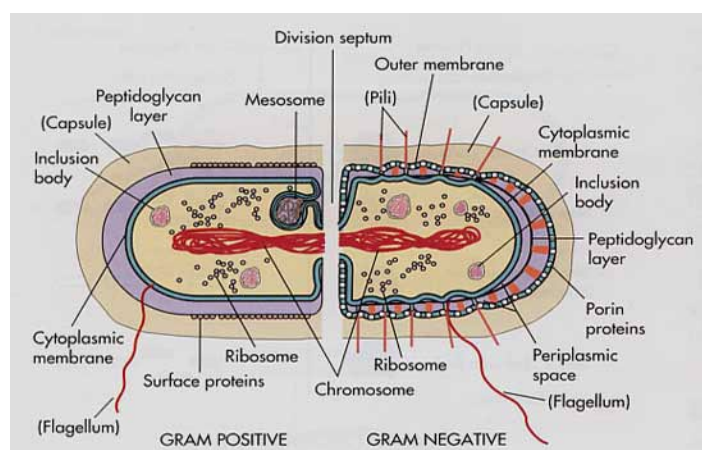
Figure 2: Schematics of the internal and external structure of a Gram-positive (left side) and a Gram-negative (right side) bacterium (digitalproteus.com)

2.2.2 Literature review

2.2.2.1 Ag$^+$ and AgNPs mechanism of action on bacteria

Silver (Ag) has been used for its antimicrobial properties since ancient times. Hippocrates was the first who used silver to his healing methods, whereas the Phoenicians used silver bottles for liquids storage to prevent spoiling (Li et al., 2010). However, silver was also used in medicine during both World Wars, and even nowadays in a variety of products in dentistry, surgical equipment and burn management (Espinosa-Cristóbal et al., 2009; Khan et al., 2011). These unique properties are due to the release of silver ions (Ag$^+$), under aerobic conditions. Under anaerobic conditions there is no Ag$^+$ release. In the following equations is the reaction of Ag with O_2:

$$4Ag\ (0) + O_2 \rightarrow 2Ag_2O \qquad\qquad (5)$$

$$2Ag_2O + 2H^+ \rightarrow 4Ag^+ + 2H_2O \tag{6}$$

Both silver ions' and silver nanoparticles mechanism of action are not yet fully understood. It is supported by several scientists that because of Ag^+ cellular proteins become inactive and DNA is unable to replicate properly. Furthermore, Ag^+ treatment leads to protein denaturation, due to the affiliation between Ag^+ and the functional groups of proteins (Sondi and Salopek-Sondi, 2004).

The way that nanoparticles act against bacteria, divide the scientific community. Stoimenov et al. (2002) explained that the nanoparticles' interaction with the *E.coli* bacteria is due to an electrostatic attraction, because the overall charge of the bacteria is negative and the nanoparticles' charge is positive. However, although Sondi and Salopek-Sondi (2004) used the same bacteria, their particles were negatively charged, but they still interacted with the bacterial membrane causing severe damages and eventually cell death.

2.2.2.2 AuNPs mechanism of action on bacteria

Gold (Au) is not affected by air and moisture, so there is no Au^+ release. Several mechanisms of action for gold are suggested; it can react with thiol groups to inhibit the interaction of degradative enzymes, and decreases the cytokine levels (Fricker, 1996).

Elsome et al. (1996), tested the antibacterial properties of a gold/polymer (JM1796) against Methicillin resistant *Staphylococcus aureus* (MRSA), *Enterococcus faecalis*, *Proteus mirabilis*, *Pseudomonas aeruginosa* and *Candida albicans*. At low concentrations, JM1796 was highly effective against *S. aureus* MRSA, *E.faecalis*, *P.mirabilis* but less effective against *P aeruginosa* and *C.albicans*.

Cui et al., (2012), suggest that there are two different mechanisms with which gold nanoparticles' can affect bacteria. The one is to affect part of the ribosome, the organelle where the proteins are produced. If a disruption in the protein production is occurred, all the cellular functions are affected. The other way is to inhibit the ATP synthesis and causing the cells' metabolism to decline. ATP is a macromolecule that provides the cell with the essential energy to complete all its processes.

2.2.2.3 Ag^+ toxicity on bacteria

A plethora of studies try to distinguish the Ag^+ from the AgNPs toxicity. Zhao and Stevens, (1998), used silver nitrate for investigating the bactericidal effects of the Ag^+ on *E.coli*. They measured different parameters, such as the initial inhibitory concentration, the complete inhibitory concentration, the postagent effect, the minimum bactericidal concentration, the maximum tolerant concentration and the log killing time. From these experiments they derived a dose response relationship; at low concentrations growth inhibition and rapid killing activity were observed. Also, when the bacterial density was increased, the ratio silver ion per cell was decreased.

In another study (Feng et al., 2000), they tested the antibacterial activity of Ag^+ on *E.coli* and *S.aureus*. After being treated with Ag^+ the bacteria exhibited similar structural changes. In

E.coli cells a big gap between the cytoplasm membrane and the cell wall was observed, whereas in *S.aureus* the cytoplasm membrane shrank and detached from the cell wall. Nevertheless, *S.aureus* remained integral, suggesting a higher resistance in Ag^+. Also, a condensed form of DNA in the center of the electron-light region in the cells was observed.

In addition, Yamanaka et al., (2005) treated *E.coli* cells with 0- and 900-ppb silver ion solutions. After 24 h of incubation, the colonies of the cells at the 0-ppb samples were stable in number, whereas at the 900-ppb samples their number was significantly reduced. In this study it is also suggested that the effects of Ag^+ are due to their interaction with the ribosome and the subsequent results in the production of enzymes and proteins, that occur because of this interaction.

2.2.2.4 Antimicrobial properties of AgNPs on E.coli

Engineered AgNPs

Choi, et al., (2008) used *E.coli* and nitrifying bacteria. It was observed that AgNPs (0.1-1 mg/L) (average size 14 nm) prevented better the nitrifying bacterial growth than Ag^+ and AgCl, whereas for the *E.coli* the Ag^+ were more toxic and no inhibition was observed below 1 μM of AgNPs concentration.

In another study (Sotiriou and Pratsinis, 2010), *E.coli* and nanosilver on nanostructured silica were used. The reason that AgNPs (4-15 nm) were immobilized on the silica is to avoid the particles' flocculation on bacterial suspension. Pure SiO_2 exhibit the same results as the control ones, so it does not influence the bacterial growth. They showed that when the size and the concentration of AgNPs (1, 6, 10, 25 and 50 wt%) were decreased, the bactericidal effect was increased. The Ag^+ release ratio was bigger for the smaller particles.

Sondi and Salopek-Sondi (2004), investigated the antibacterial effects of silver nanoparticles (average size 405 nm) against *E.coli,* using different media. When the bactericidal tests were performed on Luria-Bertani (LB) agar plates at a concentration of 10 μg/cm³, the bacterial growth was inhibited by 70%. At 20 μg/cm³ the colonies mostly were found at the edges of the plates and at a concentration of 50-60 μg/cm³ the bacterial growth was inhibited by 100%. When the tests were performed in liquid LB medium at all concentrations (10, 50, 100 μg/cm³) a growth delay was observed; as the concentration increased, the delay was increased. With TEM analysis, serious damaged was observed at the cell walls of the cells treated with AgNPs and some nanoparticles managed to penetrate into the cells.

Cho et al., (2005) used AgNPs (average size 10 nm) and platinum nanoparticles (PtNPs, average size 3 nm) coated with poly-(*N*-vinyl-2-pyrrolidone) (PVP) to assess the bactericidal effects on *E.coli* and *S.aureus*. The concentrations used were 0, 5, 10, 50, 100 ppm for both NPS. The results demonstrated that *E.coli* was more sensitive compared to *S.aureus* for both types of nanoparticles. Almost all cells were severely damaged and the surface of the cell walls was disrupted when treated with coated nanoparticles. It is known that silver releases ions but platinum is not oxidized in the air and since for both metal nanoparticles the effects

were about the same, this may indicates the distinguish between ion toxicity and nanoparticles toxicity.

Additionally, similar results were found in other studies. Spherical zero-valent AgNPs (9.2 nm) and partially oxidized AgNPs (62 nm) with concentrations 1, 3, 10, 30, 100 μg/mL were synthesized borohydride reduction of Ag+ ions (Lok, et al., 2007). It was shown that *E.coli* cells treated with partially oxidized AgNPs were significantly affected in the colony formation, compared to cells treated with zero-valent ones. The same effect was observed with the ATP levels within cells treated with oxidized AgNPs, it was decreased more than 90%, whereas within cells treated with reduced AgNPs the ATP levels were similar to that of the control. Also, another test was performed, to see if the bactericidal activities of oxidized AgNPs were affected by the diameters of the particles. They showed that the small size AgNPs were more toxic than the larger ones. The explanation of that might be the larger surface area that smaller particles have and thus, there are higher concentrations of Ag^+ or that smaller particles can more easily interact with the bacteria.

Pal et al., (2007) investigated the effect of the shape of AgNPs on their bactericidal effects against *E.coli*. They used spherical (39 nm), rod-shaped (16 nm), truncated triangular (40 nm), spherical AgNPs with an initial bacterial concentration and silver in the form of $AgNO_3$, with approximately the same concentrations (1, 6, 12, 50, 100 μg of nanosilver in 100 mL nutrient broth). The growth delay increased, as the concentration increased. Truncated triangular NPs almost completely inhibited the bacterial growth at 1 μg and the spherical ones at 12 μg reduced the colonies significantly. As the initial bacterial concentration was reduced the spherical nanoparticles exhibited higher antibacterial effects at a specific dose. Truncated triangular nanoparticles exhibited higher bactericidal properties than the spherical ones, which exhibited higher antibacterial effects than $AgNO_3$.

Additionally, in another study (Kim et al., 2007), AgNPs with mean diameter 13.4 nm were tested on *E.coli, S.aureus* and yeast with different concentrations (0.2, 0.4, 0.8, 1.6, 3.3, 6.6, 13.2, 26.4, 33 nM). AgNPs were found to be more effective in inhibiting the growth of *E.coli* than *S.aureus* and yeast, as the concentration decreased. A possible reason for the bactericidal effect is the formation of free radicals from AgNPs which induce damages to the cell membranes.

Bae et al., (2010) studied the toxicity of AgNPs in different concentrations, sizes and ionic ratios against *E.coli*. The AgNPs having diameters of 10, 22, 42, 71, 110 and 323 nm were suspended in liquid media at concentrations 25, 37.5, 50, 62.5, 75 mg/L. The researchers observed that *E.coli* inactivation was increased with increasing the concentration. A combination of AgNPs and Ag^+ was found to be more toxic than the AgNPs and Ag^+ alone. In addition, as the agglomeration rate was increased, the toxicity was decreased. Also morphological abnormalities were obvious, such as partial loss of outer membrane and localized or complete separation of the cytoplasm from the cell wall.

In another study, AgNPs (average size 5 nm) were used to study their antibacterial activity against *E.coli* (Li et al., 2010). The minimum inhibitory concentration was 10 μg/ml and as

the concentration of AgNPs increased (0, 1.25, 2.5, 5, and 10 µg/mL), the activity of membranous enzymes was decreased. Also, severe damages were obvious on the surface and the membrane of the cells exposed to AgNPs, and some parts of the bacteria were almost disorganized.

Furthermore, bactericidal activities of colloids AgNPs (8.2 and 31.1 nm) were tested against *E.coli*, *Shigella sonnei*, *Proteus vulgaris, Bacillus megaterium* and *S.aureus* (Chudasama et al., 2010). The minimum inhibitory concentrations were 100, 215, 300, 275 and 350 µg/mL, respectively. The most resistant was *S. aureus*, followed by *P. vulgaris, B. megaterium, S. sonnei* and the most sensitive was *E.coli.*

In addition, the bactericidal effects of AgNPs (size < 150 nm) were investigated after coating them with four types of surfactants (NaDDBS, SDS, TW80, CTAB) and four types of polymers (PVP, PAA, PAH, CMC) (Bae et al., 2011). The concentrations of AgNPs coated with surfactants were from 0.1 to 10 mM and of AgNPs coated with polymers were from 0.001 to 0.1 mM. The most effective were the AgNPs coated with cationic organic materials (CTAB and PAH) resulting in the lysis of the *E.coli* cells. A possible explanation for CTAB and PAH stronger effect is that they were positively charged while the surface of the bacteria is negatively charged. It was observed that the CTAB-coated AgNPs were inhibited the bacterial growth even at low concentrations and the antibacterial properties of PAH-coated AgNPs were heightened compared to the properties of AgNPs and PAH alone. TW80 and CMC coated AgNPs induced no toxic effects in the bacteria cells and SDS did not accelerate the bactericidal effect.

The antibacterial effects of AgNPs (average size 10 nm) were tested against *E.coli* and *Bacillus subtilis* with three different methods (Kim, et al., 2011); the growth inhibition assay (concentrations: 0, 10, 30 and 50 mg/L), the colony forming unit assay (concentrations: 0, 1, 5 and 10 mg/L) and the liquid-to-plate assay (concentrations: 0, 0.025, 0.05 and 0.25 mg/L). The growth inhibition assay showed that for both bacteria the inhibition was dependent on the AgNPs concentrations and serious disruptions of the cell membrane and damages in the center of the cell were observed, respectively. In the colony-forming unit, the AgNPs inhibited the formation of the colonies on *E.coli,* whereas for the *B.subtilis* this effect was not strong. At the liquid-to-plate assay the results were reverse; *B.subtilis* was more sensitive than *E.coli*. Also, some experiments were exhibited for the assessment of the toxicity of silver ions, but no toxic effects were obvious during the growth inhibition assay whereas at the colony forming unit the inhibition was 40% and 100%, respectively.

Using a different method Rattanaruengsrikul et al., (2011) investigated the antibacterial effects of AgNPs that have been formed from AgNO$_3$ in gelatin hydrogel pads against *E.coli, S.aureus* and *P.aeruginosa*. The AgNO$_3$ loading in the gelatins was differentiating (0.75, 1, 1.5, 2 and 2.5 wt %). The size of the particles was increasing as the concentration of the AgNO$_3$ increased (7.7, 8.7, 9, 9.9 and 10.8 nm in respect with the concentrations). The most sensitive was *P.aeruginosa,* followed by *S.aureus* and *E.coli*. This effect was increased as the initial amount of AgNO$_3$ in the gelatin was increased.

In a recent study, Xiu et al., (2012), used three different sizes of glycol-thiol-coated AgNPs (PEG-AgNPs), 3, 5 and 11 nm, to test their bactericidal properties against *E.coli* and the tests take place in both aerobic and anaerobic conditions. This coating does not inhibit the oxidation and subsequently Ag^+ can be released. It was shown that when the nanoparticles were stored in anaerobic conditions, Ag^+ were not present and the effect against *E.coli* was not measurable even at significantly high concentrations (158-195 mg/L). When the tests took place under aerobic conditions the effects were immediately obvious. So, they concluded that the bactericidal effects of AgNPs were due to the Ag^+. AgNPs' properties can affect the toxicity by indirect mechanisms that influence the Ag^+ release rate.

Guzman et al., (2012), investigated the bactericidal effects of four different sizes AgNPs (10, 15, 25 and 30 nm, approximately) against four different bacteria (*P.aeruginosa, E.coli, S.aureus* and *S.aureus* MRSA). These AgNPs were stabilized with sodium dodecyl sulfate (SDS). The concentrations used were 0.66, 0.89, 1.05 and 1.19 mg/L. For the evaluation of bactericidal effect they used the Kirby-Bauer method. It was observed that the bacterial growth was almost completely inhibited by the particles. As the size of the particles was decreasing, the minimum inhibitory concentrations were decreasing.

Radzig et al., (2013) used three different bacteria, *E.coli, P.aeruginosa,* and *Serratia proteamaculans* for assessing the antibacterial activities of AgNPs (average size 8.3 nm). The AgNPs concentrations were 4–5 g/mL, 10 g/mL and 10–20 g/mL, respectively. The antibiotics ampicillin, kanamycin, tetracycline, gentamicin and rifampicin were added to the medium. They assessed the inhibition of biofilms production on the bacteria. The most sensitive bacteria against nanoparticles were *E.coli* followed by *P.aeruginosa, P.chlororaphis* and *S.proteamaculans*. The MIC[AgNPs]/MIC[AgNO₃] ratio is different for these bacteria and this indicates that bactericidal properties are not completely explained by the release of Ag^+.

Morones et al., (2005) synthesized AgNPs (1-10 nm) inside a carbon matrix and tested them against *Salmonella typhi, E. coli, Vibrio cholera* and *P. aeruginosa*. The concentrations used were 0, 25, 50 and 100 μg/mL. *E. coli* and *S. typhi* were more sensitive than *V. cholera* and *P. aeruginosa* when treated with AgNPs. However, when the concentration increased more than 75 μg/ml, none of the bacteria strains exhibited any significant growth (no colonies were observed). Following microscopic analysis, nanoparticles were found all over the bacteria, not only on their surface, and it was found that these nanoparticles were smaller than 10 nm. Lastly, there is a release of Ag^+ and they have an additional contribution to the toxic effects of AgNPs.

Furthermore, *Bacillus pumilus*, a bacteria strain known for its high resistance to environmental stresses, was used for the assessment of AgNPs (polydisperse NPs, 10-40 nm) bactericidal activities (Khan et al., 2007). The concentrations used were 0, 10, 25, 50, 100 and 200 mg/L. No inhibition zone was observed with the disc diffusion test or with the agar well diffusion method. In all tested media, the AgNPs exhibited no toxic effects against *B.pumilus*.

Chlamydomonas reinhardtii is green algae which is widely used in toxicity experiments because of its short generation time, its reproduction which can be both sexually and asexually and its presence as both a heterotrophic and an autotrophic organism. Navarro et al., (2008) investigated AgNPs (10-100000 nM) and $AgNO_3$ (100-10000 nM) toxic effects on how the procedure of photosynthesis is affected. The NPs were polydispersed (10-200 nm). It was demonstrated that as the concentrations were increased the photosynthetic yield was decreased. However the toxicity was completely abolished when cysteine was added, because it reduces silver's bioavailability. Cysteine is an amino acid, essential for the cells, and is proved to be a strong ligand of Ag^+.

Pseudomonas fluorescens is a bacteria strain found in soil and water and it is unusual to cause any disease to humans. It was tested in six different growth conditions, two different exposure times and four different concentrations (2, 20, 200, 2000 ppb) against SRHA coated AgNPs (30-50 nm), latex NPs and $AgNO_3$ (Fabrega, et al., 2009). After 3 hours incubation, $AgNO_3$ found to be more toxic, followed by AgNPs and latex NPs, whereas after 24 hours AgNPs inhibited 90% of bacterial growth only in the highest concentration (2000 ppb).

Also, Espinosa-Cristóbal et al. (2009) used *S.mutans* to assess the bactericidal properties of three different sizes of AgNPs. The results demonstrate that the smaller nanoparticles, 8.4 nm, were more toxic than the 16.1 and 98 nm. The minimum inhibitory concentrations for each size were 102, 146 and 321 μg/mL, respectively. The cell membranes of the bacteria treated with all different sizes were intact.

Furthermore, synthesized AgNPs (10-20 nm) *in situ* in dental and medical resins, were tested against *S.mutans* (Fan, et al., 2011). The concentrations were 0.002, 0.01, 0.02, 0.1 and 0.2% silver. The results showed that 0.5% silver containing resin inhibited significantly the bacterial growth and even resins containing less silver (0.2%), inhibited more than 50% the bacterial growth.

Biosynthesized AgNPs

Apart from the different methods for producing engineered nanoparticles, there is a way to synthesize AgNPs from microorganisms. Specifically, *Klebsiella pneumoniae* was used for the synthesis of AgNPs (average size 22.5 nm) and combine them with different antibiotics; they tested the antibacterial activities against *E.coli* and *S.aureus*. Kirby-Bauer method was used for assessing the toxicity. The results demonstrated that AgNPs increased the bactericidal effects of penicillin G, amoxicillin, erythromycin, clindamycin and vancomycin for both types of bacteria. This effect was stronger for the *S.aureus* than for the *E.coli* (Shahverdi, et al., 2007).

In another study (Devi and Bhimba, 2012), biosynthesized AgNPs (10-20 nm) using *Hypnea sp.* and assess their toxicity against *E.coli, S.aureus* and human colon cancer cells (HT29) using different concentrations (for the bacteria: 5, 10 and 15 μg/mL, for the cancer cells: 0.156, 0.312, 0.625, 1.25, 2.5, 5 and 10 mg/mL). It was observed that the particles were more effective against *E.coli* than *S.aureus* and a potential cytotoxic activity against colon cancer cells.

S.aureus, bacteria usually found on skin, was used for biosynthesis of AgNPs (160-180 nm) against methicillin-resistant *S.aureus* (MRSA), methicillin-resistant *Staphylococcus epidermidis* (MRSE), *S.pyogenes*, *S.typhi*, *K.pneumoniae* and *V.cholerae*. The size range could not be controlled by varying the conditions during synthesis. The method used for the toxicity assessment was the Kirby-Bauer method. The most sensitive bacteria were MRSA followed by MRSE and *S.pyogenes*. The least sensitive bacteria were *S.typhi* and *K.pneumoniae* and *V.cholerae* which exhibited no inhibition zone (Nanda and Saravanan, 2009).

Dried fruits from *Tribulus terrestris* after a proper treatment, were used for AgNPs synthesis (Gopinath et al., 2012). This plant's extracts have been used for a long time in Chinese and Indian medicine, since it is known to treat several diseases. The AgNPs were found to be spherical in size and their average size was 22 nm. Their bactericidal properties were excellent against *Streptococcus pyogens, S.aureus, B.subtilis, P.aeruginosa* and *E.coli*.

Furthermore, extract from the roots of *Trianthema decandra* was used for the synthesis of Au and AgNPs (Geethalakshmi and Sarada, 2012). *Trianthema decandra* is a weed in abundance all over India. The synthesis required 3 and 6 hours for Au and AgNPs, respectively. After characterization, the AuNPs' sizes were 33.7-99.3 nm and their shape was spherical, triangular, hexagonal and cubic, whereas the AgNPs' sizes were 36-94 nm, and their shape was spherical. Both Au and AgNPs exhibited excellent bactericidal effects against *Y.enterocolitica*, *P.vulgaris*, *E.coli*, *S.aureus* and *S.faecalis*, whereas moderate bactericidal activities exhibited against *P.aeruginosa*, *B.subtilis* and *C.albicans*. AgNPs was found to have higher antibacterial effects than AuNPs.

Polyalthia longifolia is an indian native tree used for reducing the noise pollution. Kaviya et al., (2011), used the leaves extract from this tree, to produce AgNPs. The biosynthesized AgNPs were spherical and as the temperature was increasing the AgNPs did not make aggregates. The concentrations were 10^{-3} and 10^{-4} M. Their size was from 15 to 50 nm. Their antimicrobial activities were used against *E.coli, S.aureus* and *P.aeruginosa*. It was observed that the smaller NPs had higher antibacterial properties compared to the larger ones. The bigger inhibition zones were observed to *S.aureus*, followed by *P.aeruginosa* and *E.coli*.

Table 1: Summary of the literature review for the AgNPs.

Reference	Bacteria	Particle size	Concentration	Conclusions
Choi, et al., 2008	*E.coli* and nitrifying bacteria	14 nm	0.1-1 mg/L	Nitrifying bacteria growth prevented
Sotiriou and Pratsinis, 2010	*E.coli*	4-15nm	1, 6, 10, 25 and 50 wt%	Size and concentration decreases, antibacterial effect increases
Sondi and Salopek-Sondi, 2004	*E.coli*	405 nm	10, 50, 100 µg/cm^3	Growth delay and serious damaged at the cell walls
Cho et al., 2005	*E.coli* and *S.aureus*	10 nm	0, 5, 10, 50, 100 ppm	*E.coli* was more sensitive compared to *S.aureus*
Lok, et al., 2007	*E.coli*	9.2 nm and 62 nm	1, 3, 10, 30, 100 µg/mL	Small size AgNPs were more toxic than

				the larger ones
Pal et al., 2007	*E.coli*	16, 39 and 40 nm	1, 6, 12, 50, 100 µg of nanosilver in 100 mL nutrient broth	Growth delay increased, as the concentration increased
Kim et al., 2007	*E.coli, S.aureus* and yeast	13.4 nm	0.2, 0.4, 0.8, 1.6, 3.3, 6.6, 13.2, 26.4, 33 nM	More effective in inhibiting the growth of *E.coli* as the concentration decreased
Bae et al., 2010	*E.coli*	10, 22, 42, 71, 110 and 323 nm	25, 37.5, 50, 62.5, 75 mg/L	*E.coli* inactivation was increased with increasing the concentration
Li et al., 2010	*E.coli*	5 nm	0, 1.25, 2.5, 5, and 10 µg/mL	Severe damages were obvious on the surface and the membrane of the cells
Chudasama et al., 2010	*S. aureus, P. vulgaris, B. megaterium, S. sonnei* and *E.coli*	8.2 and 31.1 nm	MIC: 100, 215, 300, 275 and 350 lg/mL	Most resistant *S. aureus*, followed by *P. vulgaris, B. megaterium, S. sonnei* and most sensitive *E.coli*
Bae et al., 2011	*E.coli*	150 nm	Surfactants 0.1-10 mM and polymers 0.001-0.1 mM	Lysis of the *E.coli* cells
Kim, et al., 2011	*E.coli* and *B.subtilis*	10 nm	GIA: 0, 10, 30 and 50 mg/L CFUA: 0, 1, 5 and 10 mg/L LPA: 0, 0.025, 0.05 and 0.25 mg/L	Serious disruptions of the cell membrane
Rattanaruengsrikul et al., 2011	*E.coli, S.aureus* and *P.aeruginosa*	7.7, 8.7, 9, 9.9 and 10.8 nm	0.75, 1, 1.5, 2 and 2.5 wt %	Bactericidal effect was increased as the initial amount of AgNO$_3$ in the gelatin was increased
Xiu et al., 2012	*E.coli*	3, 5 and 11 nm	158-195 mg/L	Effect against *E.coli* was not measurable
Guzman et al., 2012	*P.aeruginosa, E.coli, S.aureus* and *S.aureus MRSA*	10, 15, 25 and 30 nm	0.66, 0.89, 1.05 and 1.19 mg/L	Bacterial growth was almost completely inhibited by the particles
Radzig et al., 2013	*P.aeruginosa, E.coli, P.chlororaphis* and *S.proteamaculans*	8.3 nm	4–5 g/mL, 10 g/mL and 10–20 g/mL	The most sensitive bacteria against nanoparticles were *E.coli*
Morones et al., 2005	*E.coli, V.cholera, P. aeruginosa* and *S. typhi*	1-10 nm	0, 25, 50 and 100 µg/mL	>75 µg/ml, none of the bacteria strains exhibited any significant growth
Khan et al., 2007	*B.pumilus*	10-40 nm	0, 10, 25, 50, 100 and 200 mg/L	No toxic effects
Navarro et al., 2008	*C. reinhardtii*	10-200 nm	10-100000 nM	As the concentrations were increased the photosynthetic yield was decreased
Fabrega, et al., 2009	*P.fluorescens*	30-50 nm	2, 20, 200, 2000 ppb	AgNPs inhibited 90% of bacterial growth only in the highest concentration
Shahverdi, et al., 2007	*E.coli* and *S.aureus*	22.5 nm		AgNPs increased the bactericidal effects of antibiotics
Devi and Bhimba,	*E.coli, S.aureus* and	10-20 nm	B: 5, 10 and 15	Particles were more

Reference	Organisms	Size	Concentration	Results
2012	*human colon cancer cells*		µg/mL C: 0.156, 0.312, 0.625, 1.25, 2.5, 5 and 10 mg/mL	effective against *E.coli* than *S.aureus* and a potential cytotoxic activity against colon cancer cells
Nanda and Saravanan, 2009	*S.aureus MRSA, S.epidermidis (MRSE), S.pyogenes, S.typhi, K.pneumoniae and V.cholerae*	160-180 nm		Most sensitive MRSA, MRSE and *S.pyogenes.*
Gopinath et al., 2012	*S.pyogens, S.aureus, B.subtilis, P.aeruginosa and E.coli*	22 nm		Excellent bactericidal properties
Geethalakshmi and Sarada, 2012	*Y.enterocolitica, P.vulgaris, E.coli, S.aureus, S.faecalis, P.aeruginosa, B.subtilis and C.albicans*	36-94 nm		Excellent bactericidal effects against *Y.enterocolitica, P.vulgaris, E.coli, S.aureus* and *S.faecalis*
Kaviya et al., 2011	*E.coli, S.aureus and P.aeruginosa*	15-50 nm	10^{-3} and 10^{-4} M	The bigger inhibition zones were observed to *S.aureus*, followed by *P.aeruginosa* and *E.coli*
Hernández-Sierra et al., 2008	*S.mutans*	25 nm	0.0976 to 100 µg/mL	High antibacterial properties
Espinosa-Cristóbal et al., 2009	*S.mutans*	8.4 nm, 16.1 and 98 nm	102, 146 and 321 µg/mL	Smaller particles more effective
Fan, et al., 2011	*S.mutans*	10-20 nm	0.002, 0.01, 0.02, 0.1 and 0.2%	The resins containing 0.2% silver inhibited more than 50% the bacterial growth

2.2.2.5 Antimicrobial properties of AuNPs on E.coli

Simon-Deckers, et al. (2008), showed that AuNPs (average size 37.5 nm and concentration 6 mg/mL) were non toxic against *E.coli*. There were no visible morphological modifications in the bacteria cells and the particles did not access the periplasm or the cytoplasm. The cytoplasm is the substance that fills the cells and constains all the organelles. Its role is important because it helps all the materials to move within the cell. Periplasm is found in Gram-negative bacteria and is the space between the cytoplasm and the outer membrane. The proteins and the molecules found in the periplasm are distinct from those found in the cytoplasm. In some cases particles were found in the bacterial surface. Additionally, NRK-52E and Hep-G2 are two cell lines commonly used for human liver toxicity assessments. Again the AuNPs did not induce any toxic effects in both cell lines.

S.mutans, a common bacterium that is present in the human mouth, has been used for tests with silver (from 0.0976 to 100 µg/mL), gold (from 0.192 to 197 µg/mL) and zinc oxide nanoparticles (from 3.90 to 4000 µg/mL). The sizes used were 25, 80 and 125 nm, respectively. Silver was found to have higher antibacterial properties, followed by gold and zinc oxide (Hernández-Sierra et al., 2008).

2.2.2.6 Toxic effects of Au and AgNPs on organisms and human cells

Except from bacteria, investigations on other organisms and human cells have been reported. *Daphnia magna*, a freshwater filter-feeding crustacean is broadly used in toxicity's experiments. It is an important organism in toxicity studies because it is at the bottom of the food chain in freshwater aquatic ecosystems and so, the slightest change in its population can result in population changes of other aquatic organisms. Two colloidal and one powdered form of silver nanoparticles and specific concentrations of $AgNO_3$ were tested against *D.magna* (Asghari et al., 2012). The most effective were powdered AgNPs, followed by colloidal AgNPs (mean diameter 7.96 nm), colloidal AgNPs (mean diameter 12.65 nm). The $AgNO_3$ exhibited relevant results. Nanoparticle aggregates were obvious to the external body surface. Small bubbles were observed under the carapace of *D.magna* when treated with the colloidal AgNPs. When treated with the powdered AgNPs, large amounts of a dark material were found in the gut tract of *D.magna*. This shows that *D.magna* ingested the NPs.

Moreover, human leukemia cells were used for determine the toxic properties of different types of AuNPs (cysteine and citrate-capped 4 nm particles, glucose-reduced 12 nm particles and CTAB-capped 18 nm particles). The concentrations were 0, 50, 100, 200 and 250 μM. The cysteine and glucose capped AuNPs were not found toxic, but the CTAB capped AuNPs were highly effective in the survival of the cells. When used CTAB modified nanoparticles, the toxicity was abolished, even though particles were found inside the cells (Connor et al., 2005).

Pan et al. (2007), used TPPMS/TPPTS-modified AuNPs for assessing their toxicity against HeLa cervix carcinoma epithelial cells, SK-Mel-28 melanoma cells, L929 mouse fibroblasts and mouse monocytic/macrophage cells. The size ranged from 0.8 to 15 nm. The smaller particles (1-2 nm) were found to be highly effective to all cells.

Gold nanoparticles (5, 12, 20, 30, 50 and 70nm) and CTAB-coated nanorods were used against human skin cell line, HaCaT keratinocytes. It was shown that both particles and rods were capable of penetrating into the cells. As the nanoparticles are concerned, no toxic effects were induced, as the cell viability of treated and untreated cells remained the same, whereas the nanorods were highly toxic. However, when the nanorods were further coated with PSS the toxic effects were abolished (Wang et al., 2008).

Yen et al., (2009) used AgNPs and AuNPs, in three different sizes (2-4, 5-7 and 20-40 nm) and two different concentrations (1 and 10 ppm), to assess their toxicity against macrophages (white blood cells). It was observed that after the Au treatment the cells were bigger, whereas with Ag treatment the morphological structure remained relatively same to the ones that they have not be treated with nanoparticles and AuNPs penetrated in the cells faster than AgNPs. Additionally, at the lower concentration, 1ppm, no toxic effects were obvious, but when treated with 10ppm, a decrease in the number of the cells was observed. As the size of AuNPs was decreased, the cytotoxicity was increased, while for AgNPs the difference in size did not induce a difference in cytotoxicity.

Table 2: Summary of the literature review for the AuNPs

Reference	Cells	Particle size	Concentration	Conclusions
Geethalakshmi and Sarada, 2012	*Y.enterocolitica, P.vulgaris, E.coli, S.aureus, S.faecalis, P.aeruginosa, B.subtilis* and *C.albicans*	33.7-99.3 nm		Excellent bactericidal effects against *Y.enterocolitica, P.vulgaris, E.coli, S.aureus* and *S.faecalis,*
Simon-Deckers, et al., 2008	*E.coli,* NRK-52E and Hep-G2	37.5 nm	6 mg/mL	Did not induce any toxic effects
Hernández-Sierra et al., 2008	*S.mutans*	80 nm	0.192 to 197 µg/mL	Moderate antibacterial properties
Connor et al., 2005	Human leukemia cells	4, 12 and 18 nm	0, 50, 100, 200 and 250 µM	CTAB capped AuNPs were highly effective in the survival of the cells
Pan et al. , 2007	HeLa cervix carcinoma epithelial cells, SK-Mel-28 melanoma cells, L929 mouse fibroblasts and mouse monocytic/macrophage cells	0.8 to 15 nm		Smaller particles (1-2 nm) were found to be highly effective to all cells
Wang et al., 2008	HaCaT keratinocytes	5, 12, 20, 30, 50 and 70nm		Nanorods were highly toxic
Yen et al., 2009	Macrophages	2-4, 5-7 and 20-40 nm	1 and 10 ppm	As the size of AuNPs was decreased, the cytotoxicity was increased

3. Materials and methods

This section describes the particles production methods used in the experiments (section 4.1), and the details of the toxicity experiments.

3.1 Particle production

Nanoparticles synthesis was performed at the Department of Chemical Engineering of Delft University of Technology. Two methods were used, the vaposization-condensation technique and the spark discharge technique. Since, one of the main objectives of this thesis is to study the toxicity of nanoparticles as a function of their size, the different parameters that can be tuned to control particle production are discussed here.

3.1.1 Vaporization-condensation technique

Condensation is the process in which particles are formed and is the basic source of aerosol in nature. Usually is required a supersaturated vapor and small particles or ions, that will lead to the nanoparticles' formation (Hinds, 1999). In the vaporization-condensation technique, vapors of bulk materials are produced by heating at high temperatures (of the order of 1000 ºC for metals). The resulting vapors are subsequently supersaturated by colling; particles are formed through process of nucleation and coagulation. Tube-furnaces are typically used to heat up the materials to produce the vapors. A constant flow of an inert gas carries the vapors away from the furnace and upon gradual cooling these vapors nucleate to clusters and nanoparticles. Inside these furnaces there is a ceramic tube, which is resistant to high temperatures, so that the vapors in the gaseous stream are only from the material being used.

High furnace temperature results in the synthesis of larger particles due to the fact that more material evaporates. On the other hand, larger flow rates through the system decrease the agglomeration time of the particles and smaller particles are synthesized. Coagulation is the process in which the particles collide with one another because of relative motion between them, and create larger particles. With this process the concentration is decreasing and the particle size is increasing. This term was usually used for particles in liquids. For solid particles, the process is called agglomeration where particles form clusters and are called agglomerates. So, when having low flows, the particle need more time to move away from the chamber that are produced and the agglomerates become bigger (Hinds, 1999).

Furthermore, the temperature and flow rate of the furnace can also affect the synthesis of the particles, since they affect the oxidation process. With slow flow rates and high temperatures, the particles have time to interact with the traces of oxygen present in the gas, and depending on the material used, ions are released.

So, for our experiments, the temperature and flow rate of the furnace were tuned to obtain aerosol nanoparticles of different mean diameters (10, 16, 22, 30 nm). The samples for the toxicity experiments were produced by depositing the aerosol nanoparticles on a glass fiber filter (47 mm in diameter). The deposition of nanoparticles was performed by passing the

aerosol through the filter, depositing all the nanoparticles on its surface (cf. Fig. 3). Five samples with different nanoparticle concentrations (4.4, 6.6, 8.8, 17.6, 35.9 mg/m^2 of filter) were produced for every diameter.

As shown in Figure 3, the AgNPs are produced in the furnace and carried away by N$_2$ flow. When was directed through route 1, the particles flow through the SMPS system which is used for measuring their size distribution. By tuning the system's characteristics, the proper concentration and size are reached. Then, the flow changes direction (route 2) and the particles are deposited on the filters.
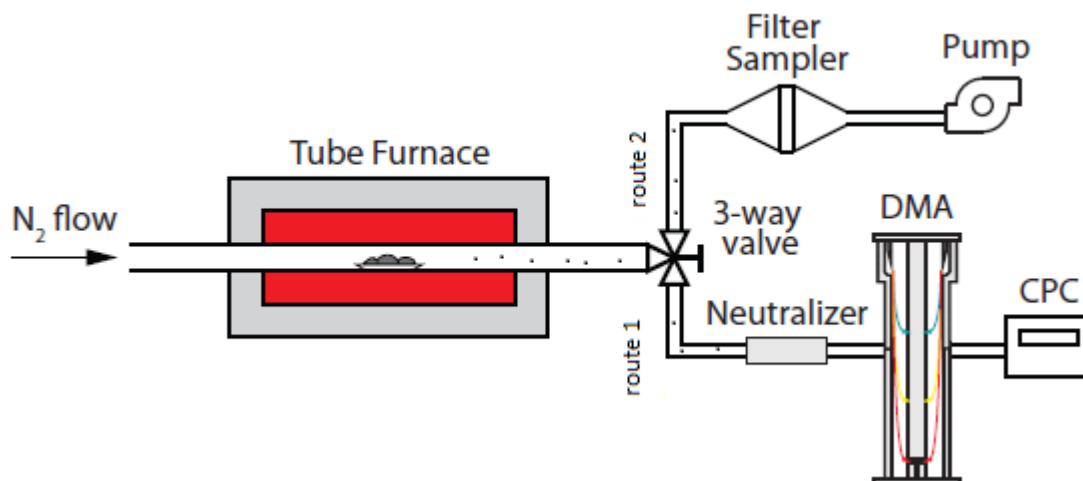

Figure 3: Schematic layout of the experimental setup used for the production of Ag ENPs with the vaporization condensation technique.

3.1.2 Spark discharge technique

The other method used for the generation of nanoparticles is with the use of the spark discharge. Two opposing cylindrical electrodes (of the material we want to make nanoparticles from connected to a constant current high voltage power supply), are placed in a few millimetres distance apart. A spark is produced between the electrodes and nanoparticles are generated.

When a low voltage is applied on a gaseous dielectric, a small current flows between the electrodes and the electrical properties of the insulation are retained (Tabrizi, 2009). But when a high voltage is applied, the current that flows through the insulation increases abruptly and an electrical breakdown takes place. This voltage is the maximum that is applied to the insulation the moment the breakdown occurs and is called breakdown voltage. The breakdown lasts a few μseconds and during that period the gas becomes conductive and plasma is generated. Plasma is called an ionized gas that contains molecules, atoms, ions, electrons and photons.

A gas breakdown is needed in order to start the spark discharge process. A conducting channel is formed, and dissociation and ionization of the gas molecules occur. A formation of a shock wave occurs because of the plasma's thermal expansion. In this short time the temperature and the pressure increase rapidly.

A conductive path between the electrodes is retained while the discharges take place. Because of this, evaporation of the cathode material is happening. This is followed by rapid cooling and because the vapor cloud is small compared to other evaporation-condensation processes, a high concentration of very small particles is formed. With this technique the material is heated locally, compared to the vaporization-condensation technique where the evaporation was taking place from all the surface area of the bulk material.

A constant flow carries away the nanoparticles from the chamber that are produced. With every discharge that occurs, energy is dissipated. This energy is defined as:

$$E = \frac{1}{2}\, C * V^2 \tag{1}$$

where C is the capacitance of the spark, and V the discharge voltage between the two electrodes.

The characteristics of the spark are quite sensitive to the shape of the electrodes and the gas composition. As the gap between the electrodes increases, the size of the particles increases, whereas higher amounts of energy are needed for the production of the same mass of NPs. The increase of the operating pressure has similar effects because of enhanced cooling. In addition, as the capacitance is increased, the size and the concentration of the particles is increased respectively (Tabrizi, et al., 2009).

For our experiments we used the spark technique for the generation of Au and AgNPs. For these experiments we kept constant the voltage of the DMA. With this, narrower size distributions were achieved, comparing to the previous method in which there were polydisperse NPS. Thus, with this method there was control on the particles' diameter.

The sheath flow passing through the DMA was 16.5 lpm on average, whereas the N_2 that flew through the whole system and carried the NPs was 5 lpm. When the particles were produced in the spark chamber, they made agglomerates. To avoid this phenomenon, an oven was used at high temperatures (990 °C), and the particles became completely spherical. With this, a total control on the morphology of the particles was achieved. An electrostatic precipitator was used for the deposition of particles on TEM grids, for their characterization. The particles were negatively charged and the voltage applied on the precipitator was positive. As the aerosol entered the precipitator, the particles were attracted and deposited on the surface of the TEM grid. The voltage used for the deposition in the electrostatic precipitator was 6KV.

The DMA's voltage was tuned manually according to the required size (for Au: 10, 20, 40, 80 nm, for Ag: 10, 20, 40 nm) (Table 3). Also, we made samples of 20- and 40-nm particles at 4

different concentrations (2.2, 4.4, 8.8 and 17.5 mg/m^2) (Table 4). The spark voltage and the frequency were tuned each time in different values, so that the maximum concentration is achieved. The total NPs surface area was kept constant for all the samples. When the surface area is the same, the ion release rate maybe the same for all the different sizes and concentrations (Wijnhoven et al., 2009). So, if there is an ion-toxicity effect it may be correlated with the silver ion release rate.

Table 3: The NPs diameters that were produced from the spark discharge technique, for the 4.386 mg/m^2 .

Element\Size (nm)	10	20	40	80
Ag	X	X	X	
Au	X	X	X	X

Table 4: The four different concentrations used, only for 20 and 40 nm Ag and Au NPs.

Concentrations (mg/m^2)	2.193	4.386	8.772	17.544
Ag 20 nm	X	X	X	X
Ag 40 nm	X	X	X	X
Au 20 nm	X	X	X	X
Au 40 nm	X	X	X	x

As shown in Figure 4, the NPs are generated in the spark and carried to the oven where they become spherical. Then, through the DMA they are size-selected. In route 2, the NPs end up directly to the CPC where their concentration is measured. When the maximum concentration is reached, the flow changes to route 3, where the NPs are deposited on TEM grids in the electrostatic precipitator for their characterization. Finally, when the flow follows the route 1, the NPs are deposited on the fiber filters for the toxicity assessment.
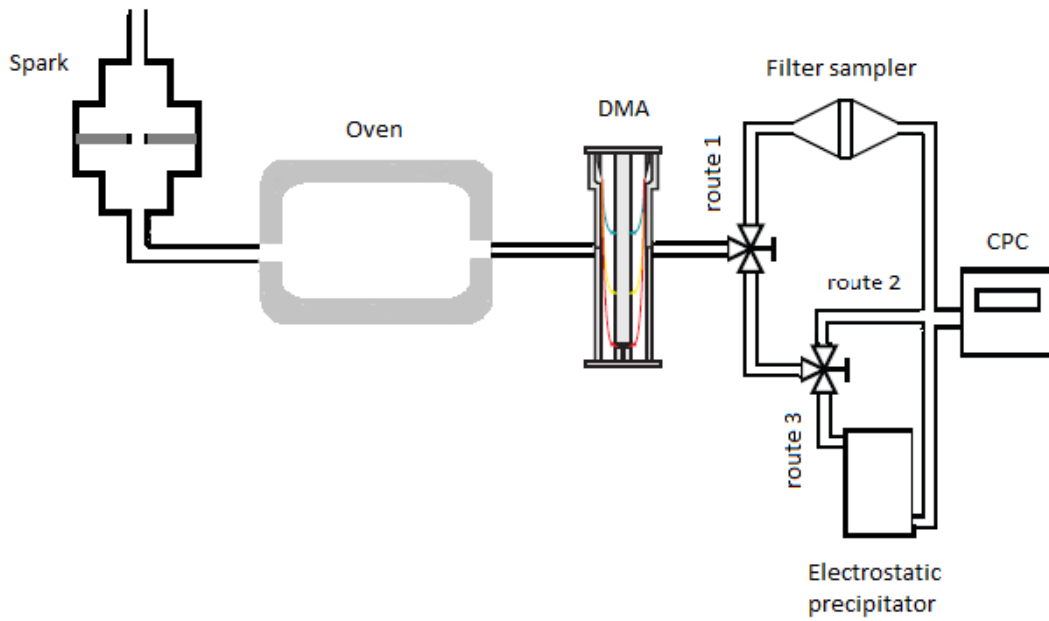
Figure 4: Schematic layout of the experimental setup used for the production of Ag and Au ENPs with the spark discharge.

Both gas-phase synthesis methods described above offer the advantage of high purity with respect to the liquids (Lehtinen et al. 2004). Moreover, other advantages are that are flexibility of the methods with respect to the material, continuous production of particles and good control over their size. They are no demanding methods, since the only thing required is the electric power (Tabrizi, 2009).

3.2 Size selection and characterization

The particles coming out of the nanoparticle sources have a broad particle size distribution (PSD). In this chapter it is explained how we can size select this aerosol with a broad PSD into a monodispersed aerosol with a very narrow PSD. Within this subchapter it also is shown how this monodispersed aerosol can be used to characterize and quantify the particles directly in the gas phase (3.2.2) or on a substrate (3.2.3).

3.2.1. Differential Mobility Analyser (DMA)

The DMA is a device where the particles are separated according to their electrical mobility. When a particle is placed in an electrostatic field, the terminal velocity that reaches due to the electrostatic force is proportional to its electrical mobility (i.e., its ability to move within an electrostatic field). That velocity is given by the following formula:

$$v = \frac{n*e*E*Cc}{3*\pi*\mu*dp}$$
(2)

where n is the number of elementary charges on particle, e is the elementary unit of charge $(1.602*10^{-19}$ C), E is the electric field strength (V/m), Cc is the slip correction factor, μ is the gas viscosity (Pa*s), and dp is the particle diameter (m).

The electrical mobility of a particle is defined as:

$$Z = \frac{n*e*Cc}{3*\pi*\mu*dp}$$ (3)

where n is the number of elementary charges on particle, e is the elementary unit of charge $(1.602*10^{-19}$ C), Cc is the slip correction factor, μ is the gas viscosity (Pa*s), and dp is the particle diameter (m).

The electrical mobility is a function of particle size, when all particles have the same number of charges. With the use of the electrical mobility particles can be differentiated according to their size. So, with the DMA specific particles' sizes can be extracted through an aerosol containing particles of different sizes (Afonso, 2007).

Figure 5 shows a schematic cross section of the DMA. Purified sheath air is introduced at the top of the column (Q_{sh}) and exits from the bottom (Q_{ex}). The role of the sheath flow is to make sure that the flow inside the tube is laminar and enter and stays at the boundaries of the outer electrode. The aerosol with the particles (Q_a) enters at the top of the tube in a perimetric flow attached to the outer electrode. From that flow only the particles with a specific electrical mobility Z_p are collected through the monodisperse particles exit at a flow Qs.

High voltage is applied on the central rod whereas the outside of the tube is grounded and an electrical field is formed. Because of the electrical field, a force perpendicular to the flow is applied, and the charged particles are drawn across the laminar flow. Depending on the voltage, only the particles with a specific electrical mobility exit the classifier, while the rest will collide with the central rod or the outer wall and the uncharged ones will go through the DMA without deviating from the aerosol flow (Knutson and Whitby, 1975). Apart from the aforementioned operating conditions the performance of a DMA is also affected by its geometry parameters (Steiner, 2011).
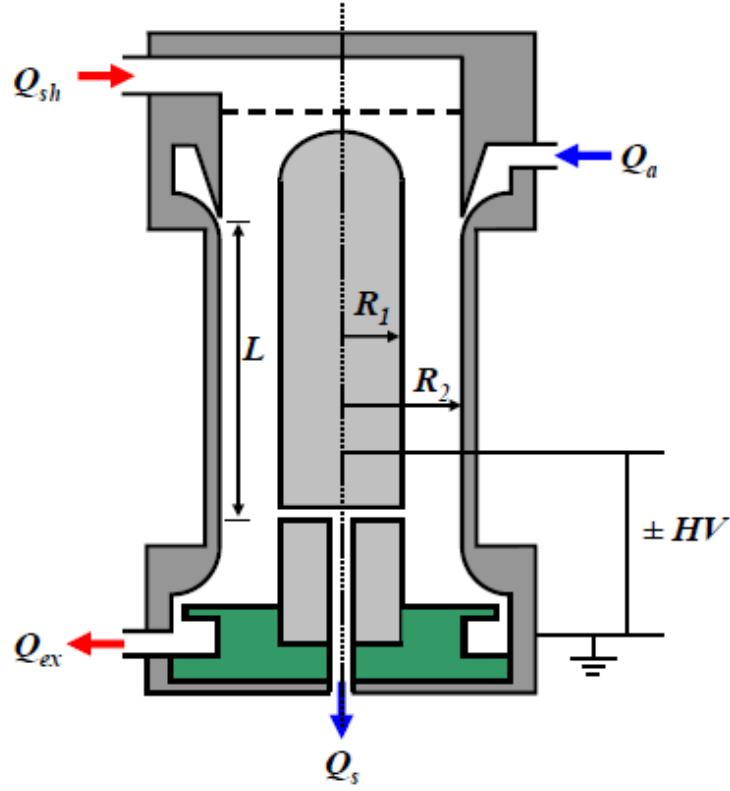
Figure 5: Schematic cross- section of a Differential Mobility Analyzer (Steiner, 2011).

The mean electrical mobility of the particles that exit the DMA is defined as:

$$Z = \frac{Qsh * \ln(\frac{R2}{R1})}{2 * \pi * L * V} \qquad (4)$$

where V is the voltage applied on the central rod, L is the effective axial distance between aerosol inlet and aerosol outlet, R_1 is the outer radius of the inner electrode and R_2 is the inner radius of the outer electrode.

The ratio of the mobility which corresponds to the peak of the transfer function to the full width of the mobility transfer function at its half maximum, is called DMA's resolution (Giamarelou, et al., 2012). According to Knutson and Whitby (1975), if the aerosol is monodisperse and the transfer function nondiffusive, the full width at half maximum can be expressed as:

$$(FWHM) = \frac{qa + qs}{qc + qm} \qquad (5)$$

where qa is the aerosol's flow, qs is the sample's flow, qc is the sheath flow and qm is the main outlet's flow.

As the resolution decreases, the size distribution becomes narrower. So, the resolution of the DMA can be expressed as:

$$R = 1/(FWHM) \qquad\qquad (6)$$

3.2.2. Scanning mobility particle sizer (SMPS)

The SMPS is used to characterize the aerosol coming out of the particle sources, directly in the gas phase. The SMPS consists of three parts: the neutralizer, the DMA and the Condensation Particle Counter (CPC).

As explained in sect. 3.2.1 the DMA can only select particles of the same size if the carry the same charge. Such distribution is achieved by passing the aerosol coming out of the particle source through a neutralizer. The neutralizers usually employ a radioactive source to produce ions which then diffuse to and stick on the particles, thereby transferring their charge to them. Only then, the aerosol is size-selected in the DMA.

The Condensation Particle Counter is used for measuring the concentration of the selected particles that exit from the DMA. Very small particles cannot be distinguished from the background noise, and thus, are not detected. So, for this to be achieved, the aerosol is mixed with alcohol in a warm chamber. Subsequently, the aerosol with the alcohol's vapors flow at a cold chamber, where the vapors become super-saturated and condense on the particles. With this procedure, the particles become bigger and are easily detected (Stolzenburg and McMurry, 1991).

3.2.3 Particle characterization on a substrate

Since the monodisperse aerosol coming out of the DMA is charged with one polarity, it can be easily deposited on a substrate by applying an electric field that attracts the particles on it. Once the particles are on the substrate, they can be characterized (morphology, composition and quantity) with microscopy methods (e.g., Scanning Electron Microscopy, SEM, and Transmission Electron Microscopy, TEM).

SEM is a device for observing nanometer-sized objects with a focused beam of high-energy electrons that generate a variety of signals at the surface of solid samples. These signals can offer a lot of information about the sample such as the morphology, the crystalline structure and the chemical composition. Accelerated electrons produced by the beam interact with the sample. From this interaction, secondary and backscattered electrons are dissipated, and imaging is feasible (Goldstein et al., 2003).

3.3 Toxicity experiments

Overall two different sets of experiments were conducted: the first one was in the 'Vostaneio' General Hospital, in Mytilene, Greece, and the second in the Bionanoscience Department of Delft University of Technology, in Delft, The Netherlands. The subsections that follow describe the steps principles and the procedures of these tests.

3.3.1 Disk diffusion susceptibility test protocol (Kirby-Bauer method)

The disk diffusion susceptibility test protocol or else the Kirby-Bauer test method for assessing bacteria's sensitivity against antibiotics, was established in 1960. The purpose of this method is to determine the sensitivity or resistance of the pathogenic bacteria to several antimicrobial compounds, so that a physician can select the proper treatment for the patient. When a filter paper disk with a known concentration of an antimicrobial compound is placed on an agar plate, the water from the agar is absorbed into the filter. As a result, the compound will begin to diffuse into the agar with the concentration being reduced as the distance from the filter increases. The depth of the agar plays an important role to the size of the inhibition zone, since the antimicrobial compound diffuses in three dimensions; a deeper layer will produce a smaller inhibition zone than a shallow one (Bauer et al., 1966). The advantages of this methods is that it is simple (no need for special equipment), quick, cheap, and has great repeatability.

3.3.2 Preliminary experiments

Part of the toxicity experiments took place in the 'Vostaneio' General Hospital in Mytilene at the Microbiology Department. The strains of the *E.coli* were taken from the hospital and the Mueller-Hinton (MH2) agar plates, were the bacteria were cultivated, were purchased from Biomerieux Hellas (Athens, Greece). The agar in the Mueller-Hinton plates contains 2.0 g bovine extract, 1.5 g soluble starch (potato), 17.5 g acid hydrolyzed casein (bovine), 17 g agar and 1 L pure water.

After the bacteria identification and reculture, they were left for overnight incubation at 37° C, so that when the bacteria will be used, they would be at the exponential growth phase. After incubation, one or two clean and isolated colonies were taken with a sterilized cotton swab and were diluted in a test tube that contained nutrient broth. Then the turbidity was measured and it should be 0.5 according to the McFarland scale, so that the inhibition zones after the incubation would be obvious. If the turbidity was less than 0.5, additional bacteria were added. If the turbidity was more than 0.5, nutrient broth was added. A sterilized cotton swab is immersed in the liquid and a coating of bacteria was placed in the MH2 agar plates.

Nanoparticle-laden filters discs 5 mm in diameter were cut out of the 47-mm filters that were prepared as described in sect. 3.2.1, and applied on top of the bacteria cultures. The surface with the particles was facing down to ensure interaction with the agar and the bacteria. Then the plates were incubated for 48 h in total. Every 12 h the plates were observed and the inhibition zone was measured with a ruler, according to the Kirby-Bauer disk diffusion susceptibility test protocol.

The inhibition zones are the area around the NP-ladden filters, were bacteria are killed because of the particles. The size of the inhibition zone is affected by diffusion rate of the tested compound, the time that this compound is left to diffuse, the initial concentration of the compound, the depth of the agar and the temperature (Humphrey and Lightbown, 1952).

 In Figure 6 two parameters that affect the diameter of the inhibition zone are plotted. The diffusion time of the compound is plotted versus the diameter of the zone (cf. Figure 6A). As the time passes the diameter of the inhibition zone increases until the 24 h were it becomes

stable. This is also proportional with the diffusivity of the tested compound. Furthermore, the distance from the center of the filter is plotted versus the concentration of an antibiotic (penicillin) (cf. Figure 6B). As there is a removal from the center towards the edge of the inhibition zone the concentration of the antibiotic decreases. It is believed that NPs and ions may follow the same pattern.
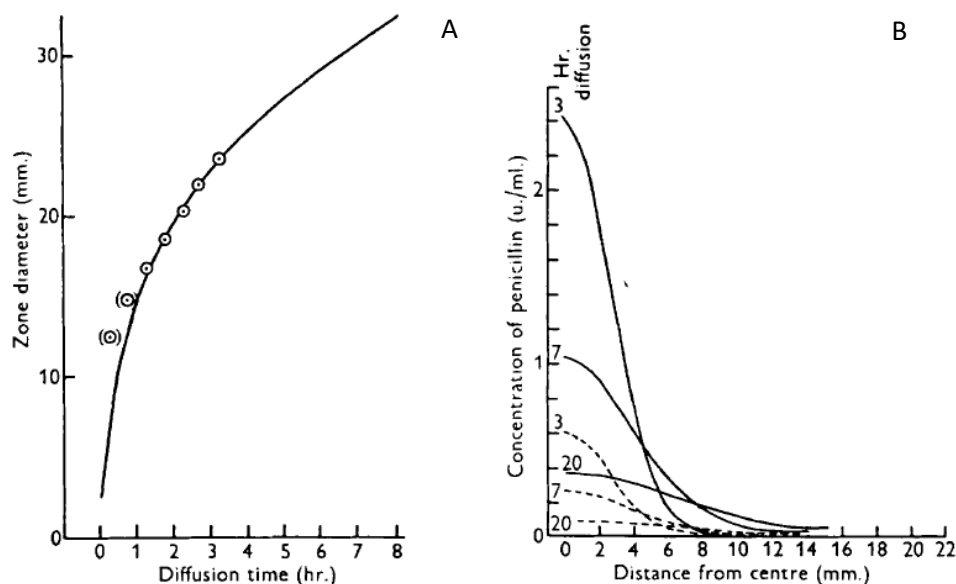

Figure 6: A) The diffusion time of the compound is plotted versus the diameter of the zone, B) The distance from the center of the filter is plotted versus the concentration of an antibiotic (penicillin) (Humphrey and Lightbown, 1952).

3.3.3 Subsequent experiments

Another set of toxicity experiments was conducted at the Bionanoscience Department, at TU Delft. The *E.coli* strain that I used in this case was the MG1655, a genome that is close to the wild *E.coli* cells and has a few interventions (University of Wisconsin, 2013). This means that this strain looks like the strains found on nature.

Three different experiments were conducted in total. The differences in these experiments were in the way the bacteria were spread on the plates and how the filters were placed on them. In the first set of experiments (cf. Figure 7), I repeated the same procedure as the one at the preliminary experiments but for two different turbidities, 0.5 and 0.25. The turbidity was measured with a spectrophotometer. For each sample 3 replicates were made.
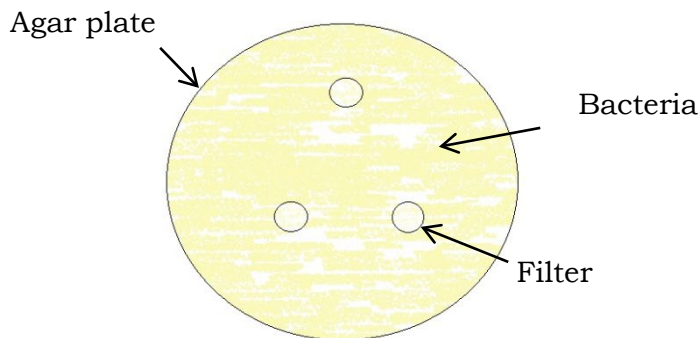
Figure 7: Schematic of the experiment where the bacteria are spread on the agar plate and the NP-ladden filter is placed on top of them, with the particles face down.

In the second experiment (cf. Figure 8), the turbidity was 1 and they were spread all over the agar plates. Filters of 20 nm Ag and AuNPs, with concentration 17.5 mg/m² were placed with the particles facing up, so that there is no direct interaction with the agar and the bacteria. A small drop of water (2 µL) was taken with a pipette and placed on top of each filter. Then, the plates were left in the incubator for 24 h.
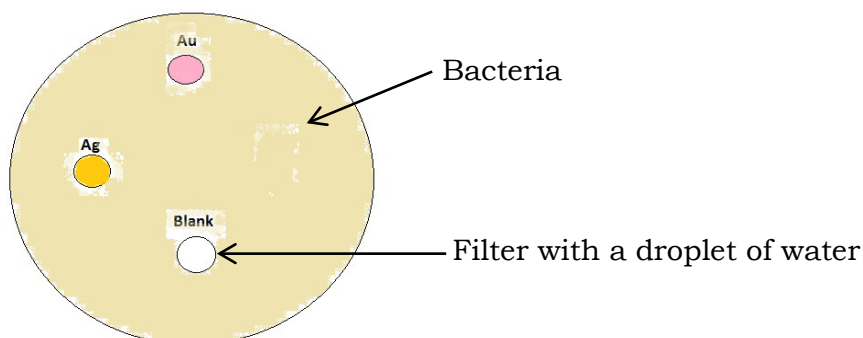

Figure 8: Schematic of the experiment where the bacteria are spread on the agar plate, the NP-ladden filter is placed on top of them, with the particles face up and a 2µl water is placed on top of the filters.

In the third experiment (cf. Figure 9), no bacteria were spread on the agar plates. The filters, with 40 nm Ag and Au NPs, with concentration 17.5 mg/m², were placed on the agar plates facing up. A 5µl bacterial suspension was placed on top of the filters and the plates were left in the incubators for 24 h.
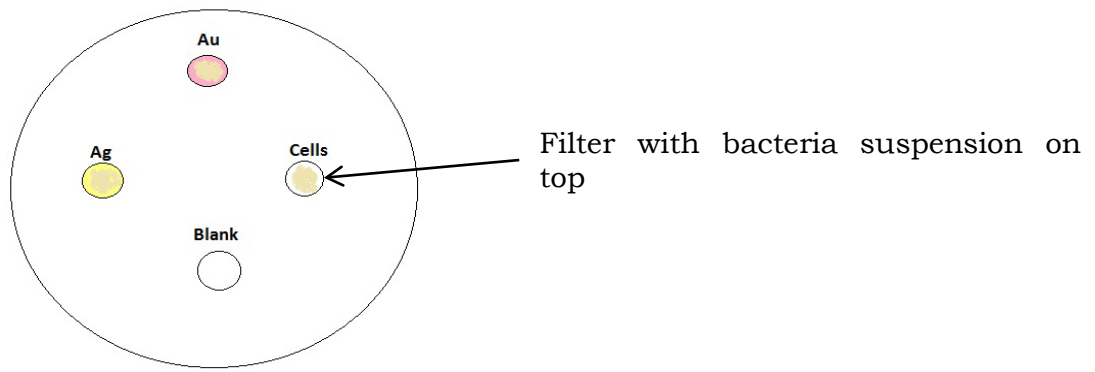
Figure 9: Schematic of the experiment where the NP-ladden filters are placed on the agar plates, the particles face up, and a 5µl bacterial suspension is placed on top of the filters.

4. Results and Discussion

4.1 Nanoparticle characterization

Two methods of imaging (SEM) were used for the characterization of the NPs generated with the spark discharge technique.

The SEM imaging was done for checking the point at which the NPs would become completely spherical. When the particles are produced, are forming agglomerates and not single particles. All the particles used for in the SEM measurements were gold and their size was 80 nm due to the limited resolving power of the microscope.

Firstly, when the oven was not in use (cf. Figure 10A), at a deposition of 1 minute, big agglomerations were obvious and single, isolated nanoparticles were not found in the samples. Thus, the actual size is lost, since the one agglomeration falls on top of the other. The only size that matters is the one that primary particles have which cannot be resolved with the SEM.

Then, when the oven temperature was increased to 375° C, at a deposition of 15 minutes, there were still agglomerates of 3-5 nanoparticles but isolated (cf. Figure 10B). The difference in the deposition time lies in the difference in the TEM grids. In the first deposition there was no film in the grid and the aerosol flow was passing through the grid, whereas in the second depositiin the grid was attached at the bottom of the electrostatic precipitator and the particles were deposited on it by diffusion.

The oven temperature increased to 680°, but still agglomerates were visible (cf. Figure 10C). At 780° C the particles were completely isolated but their size was not spherical yet (cf. Figure 10D). When the temperature reached 990°C the particles were totally rounded, because at such high temperatures the NPs' agglomerates melt and spherical NPs were formed. (cf. Figure 10E and F).
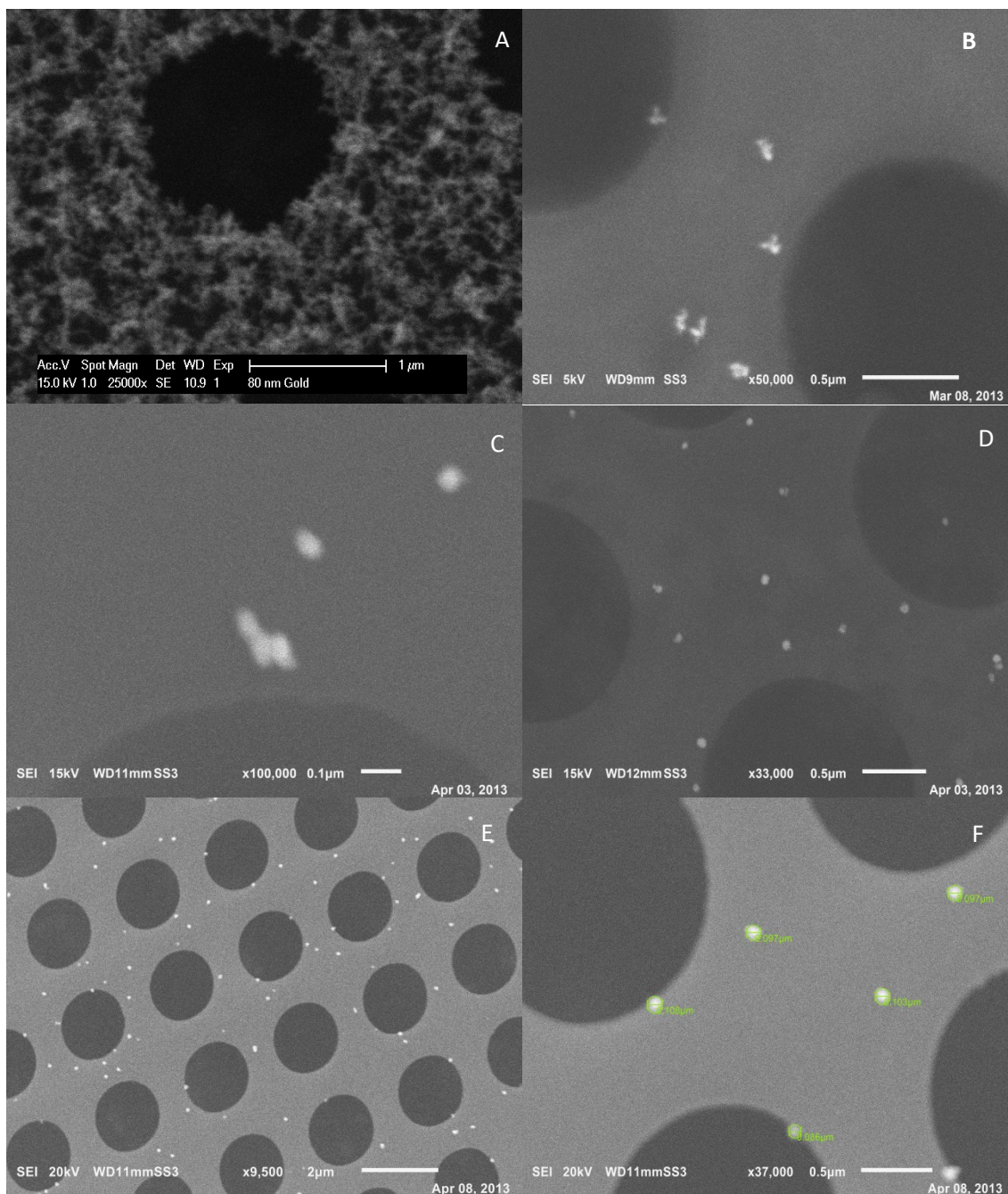
Figure 10: A) AuNPs without using the oven, B) AuNPs at 375º C, C) AuNPs at 680º C, D) AuNPs at 780º C, E) AuNPs at 990º C, F) AuNPs at 990º C, with a size distribution from 86 – 108 nm.

In Figure 11, the size distributions of the AgNPs produced with the vaporization-condensation technique are depicted. It is observed that the size distributions are quite broad, since in each sample there are particles from 6-80 nm, approximately. The diameter of the particles at which the peak occurs, has the highest concentration. So, the filters that were made, were 10 (cf. Figure 11A), 16 (cf. Figure 11B), 22 (cf. Figure 11C) and 30 nm (cf. Figure 11D).
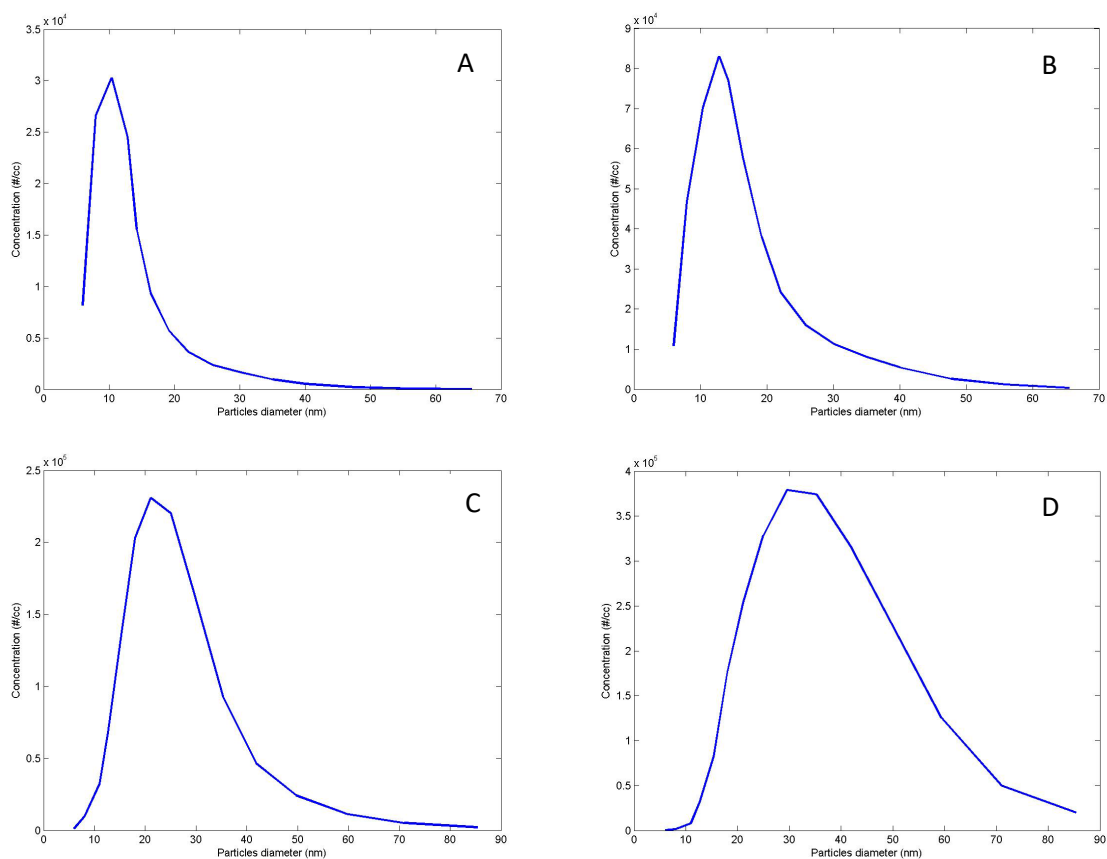
Figure 11: AgNPs size distributions for A) 10 nm, B) 16 nm, C) 22 nm, and D) 30 nm.

In Table 5, are cited the minimum, the maximum and the mean diameter of the Ag and AuNPs that were produced with the spark discharge technique according to Knutson and Whitby (1975). In these experiments the FWHM is 1/3, so the resolution is 3. The size distribution is quite narrow, compared with the particles' size distribution that were produced with vaporization-condensation technique. The spark discharge technique offers a better control to the size of the particles.

Table 5: The minimum and the maximum diameters of the Ag and Au NPs.

Mean diameters (nm)	Minimum diameters (nm)	Maximum diameters (nm)
10	8.4	13
20	16.6	26.6
40	31.1	53.7
80	65.6	110

4.2 Toxicity assessment

4.2.1 Preliminary experiments' results

Figures 11 and 12 show results from the experiments with the AgNPs produced with the vaporization-condensation technique. In these figures, the ratio of the diameter of the zones versus the diameter of the filter (dzone/dfilter) is plotted against the concentration and the diameter.

It is obvious (cf. Figure 11) that as the mass concentration increases, the dzone/dfilter ratio increases for all four different sizes. As the mass on the filter increases, the number of the particles increases. Thus, there are more particles that can release Ag^+, the diameter of the inhibition zones is bigger and so, the ratio dzone/dfilter is bigger. As far as the two highest concentrations for 10 nm no inhibition zones were exhibited. It is possible in these two filters no NPs were deposited.
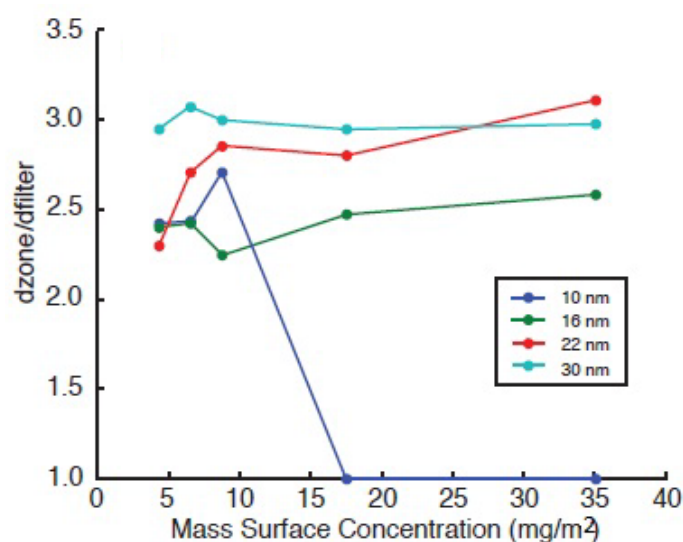

Figure 11: Growth of inhibition zones as a function of particle mass concentration.

Furthermore, as the particle size increased (cf. Figure 12), the same phenomenon was observed; as the size increases, the ratio also increases. It would be expected that the smaller particles would exhibit bigger inhibition zones because of their bigger surface area. Small particles have bigger surface area than the big particles and so, there is more space for silver to dissolve and produce Ag^+. Higher ion release would lead to greater bactericidal activity. But instead, it is observed that as the diameter of the particles increases, the effect also increases.
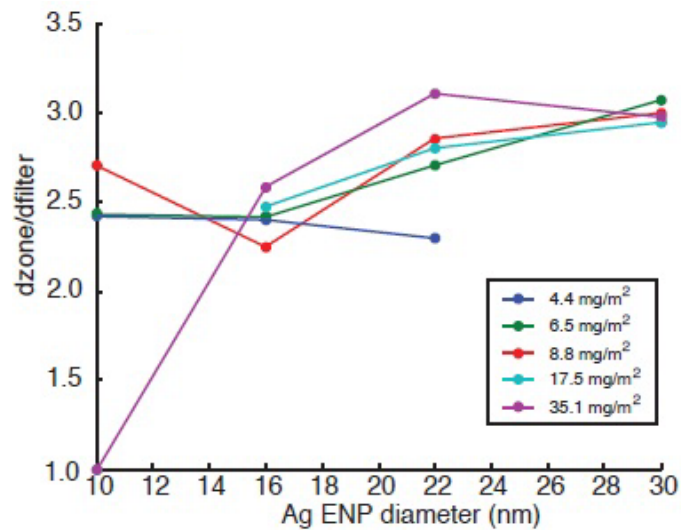
Figure 12: Growth of inhibition zones as a function of particle size.

In Figure 13, there are some pictures after 48 h of incubation. The white circles are the NP-ladden filters and the inhibition zones around them are quite distinct. In the rest of the plate the bacterial growth is visible.
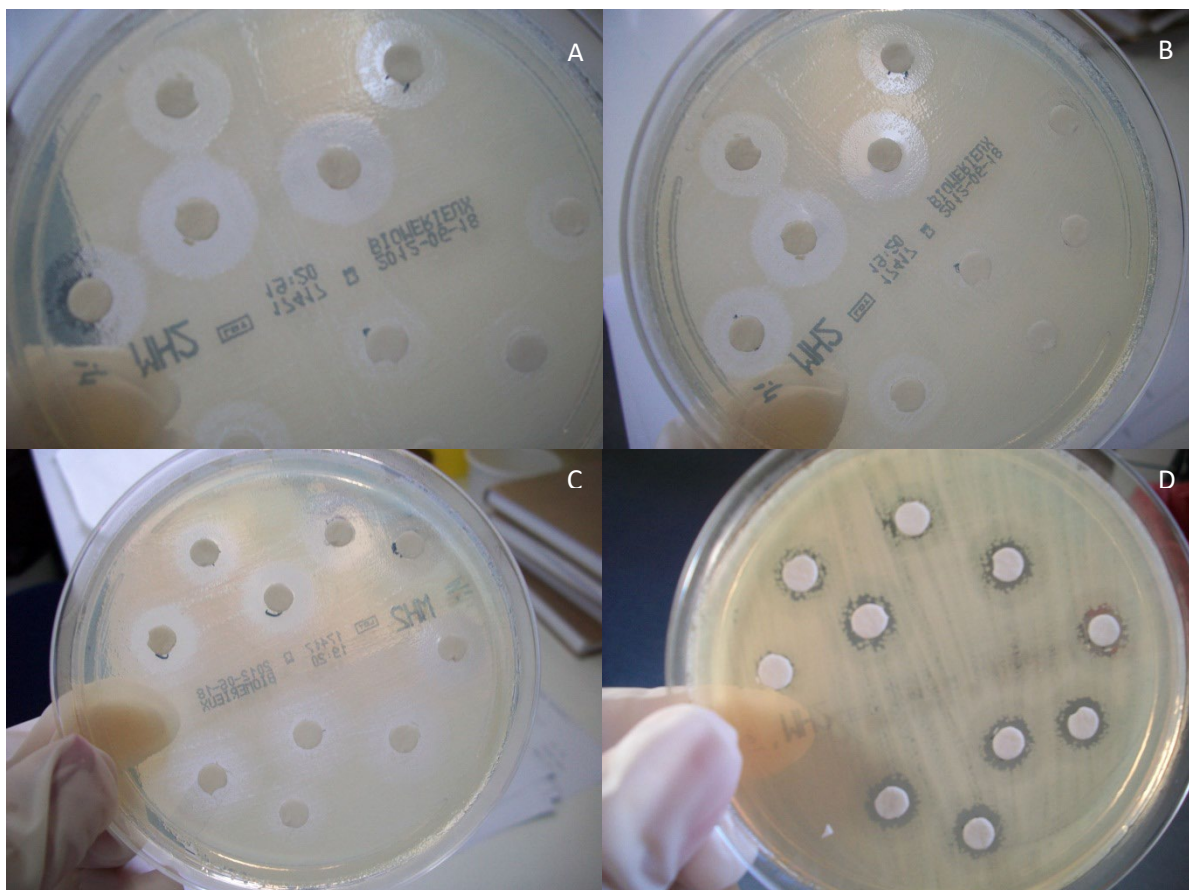

Figure 13: A), B), C) and D) The inhibition zones are easily observed.

4.2.2 Experiments conducted in TU Delft results

In Figure 14 the particles' diameter is plotted versus the dzone/dfilter ratio. For AuNPs there were no inhibition zones, indicating that there are no toxic effect for the concentrations we employed. For the AgNPs, the same diameter in the inhibition zones of all samples was observed, regardless of size and concentration. For the 80 nm AgNPs there were no filters with particles due to the time needed for their deposition. This may be an effect of the total particles' surface area that was kept constant. Since the surface area is kept constant, in all samples there is the same Ag^+ release rate and so, the antimicrobial effect is the same. Also, as the turbidity decreases, the dzone/dfilter ratio increases. When less bacteria are spread on the plates, the toxic effect is stronger.
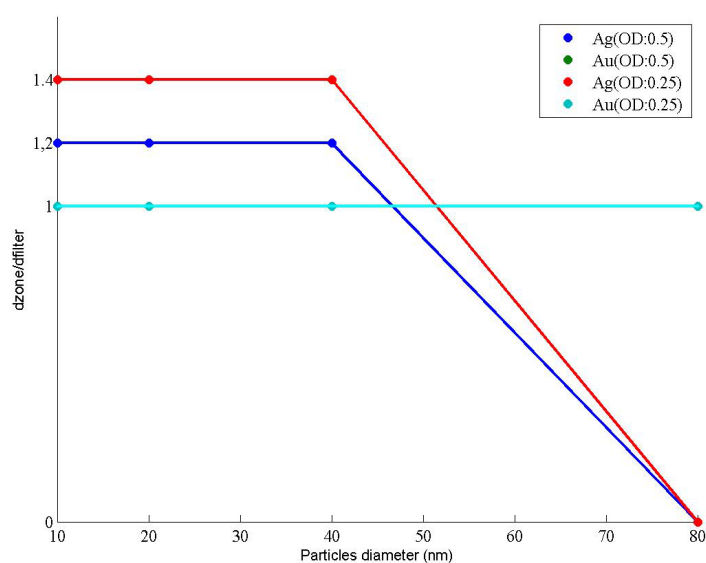

Figure 14: The particles size diameter versus the ratio dzone/dfilter. In both densities the Au NPs show no inhibition zone, as the ratio is 1. For the Ag NPs, as the optical density decreases, the ratio increases.

In Figures 15 and 16 the four different concentrations are plotted versus the dzone/dfilter ratio. For 20 nm (cf. Figure 15), AuNPs there is no inhibition zones observed, whereas AgNPs are not toxic for the lowest concentration (2.2 mg/m^2). However, for the 40 nm (cf. Figure 16), again the AuNPs are not toxic for all different concentrations, but for AgNPs only the 4.3 mg/m^2 showed inhibition zone. Such results for AgNPs were not expected since for all the samples the surface area was the same and the dzone/dfilter was the same. The procedure followed was the same for all samples and so was the incubation time. So, maybe there is another parameter that affects the antibacterial activity of 20 and 40 nm at specific concentrations. Compering with the preliminary experiments, the ratio dzone/dfilter was in all samples bigger than in these experiments.
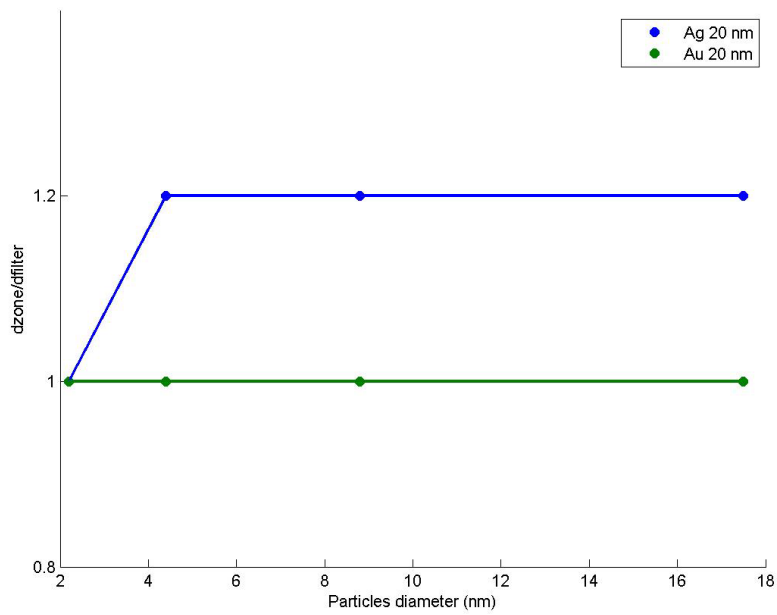
Figure 15: The concentrations versus the ratio dzone/dfilter, for the 20 nm (what turbidity is that? 0.5, 1?).
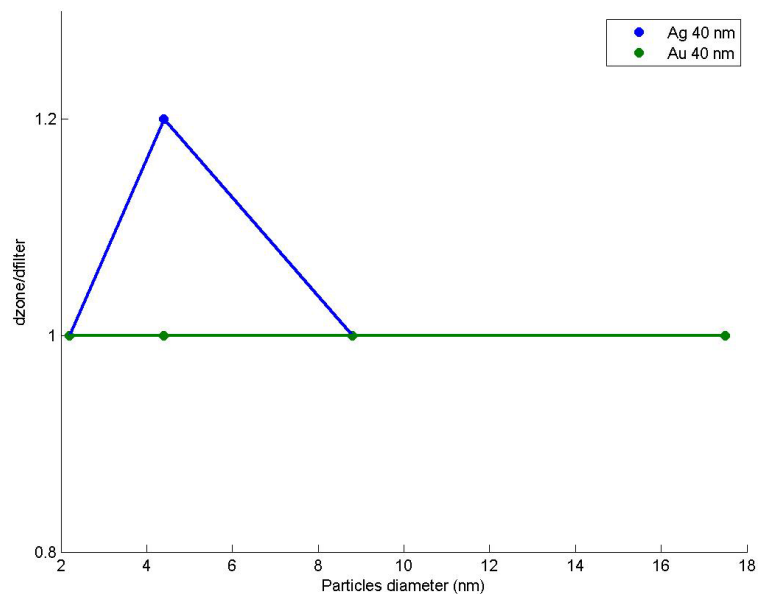
Figure 16: The concentrations versus the ratio dzone/dfilter, for the 40 nm.

In Figure 17 there are some photos from the experiments conducted in Delft. Using two different turbidities, the growth of the inhibition zones at AgNPs (cf. Figure 17B and D) is visible. For AuNPs, no inhibition zones were formed (cf. Figure 17A and C).

In these results the toxic effect is due to Ag^+ and not to NPs. If there was a nanoeffect then inhibition zones should be also observed in samples with AuNPs. Also, the inhibition zones for AgNPs were the same regardless the differences in size and concentration. Since there is no such result, the observed killing effect is due to the Ag^+ that were formed from the

interaction of AgNPs with the atmospheric oxygen. So, the parameter that affects the bactericidal activity is the surface area that was constant.
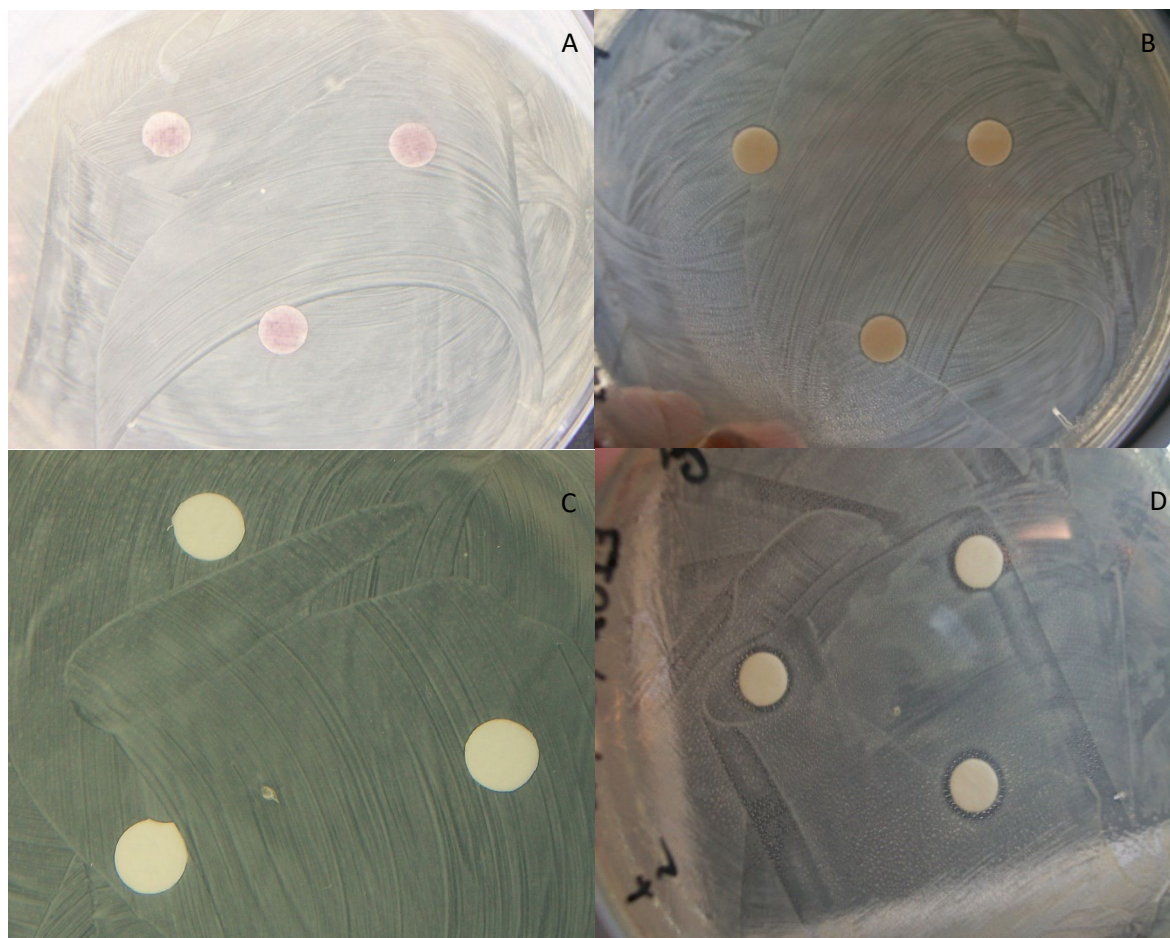

Figure 17: A) AuNPs with optical density 0.5, no inhibition zones observed, B) AgNPs with optical density 0.5, inhibition zones of 6 mm are measured in all samples, C) AuNPs with optical density 0.25, no inhibition zones observed, D) AgNPs with optical density 0.25, inhibition zones of 7 mm are measured in all samples.

In Figure 18, there are photos from the experiment with the droplet and the bacterial suspension. Only for the AgNPs there was a small inhibition zone formed around the filter (cf. Figure 18A), even if the particles did not have direct interaction with the agar and the bacteria. This shows that the droplet of water helped the diffusion of the particles. In the experiments with the bacterial suspension placed on top of filters (cf. Figure 18B), the bacterial growth on top and around the filters is visible. These samples were tested on the microscope and the bacteria were intact in all filters. This experiment should be repeated with different sizes, because the 40 nm particles exhibited no inhibition zone at the first experiments, and so these results may not be accurate.
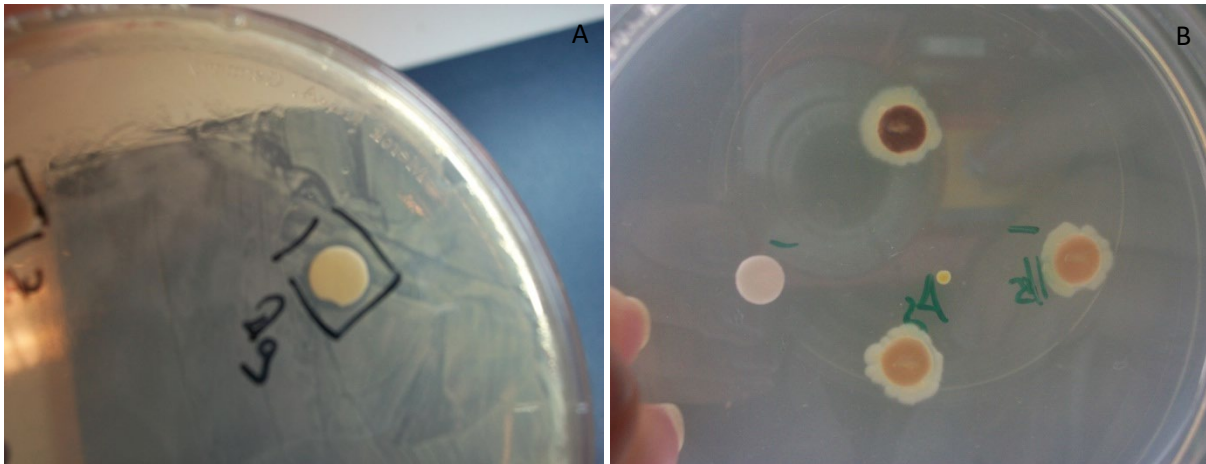
Figure 18: A) From the experiment with the droplet, a 6 mm inhibition zone was observed only in the filter where the AgNPs were deposited, B) From the experiment in which a bacterial suspension was placed on top of the filters, bacterial growth is observed on top of and around the filters.

5. Conclusions

A conclusion can be drawn that Kirby-Bauer method can be used for assessing ion and not nano toxicity. If there was a nano effect, inhibition zones should be obvious in samples with AuNPs and maybe bigger inhibition zones should be observed in the AgNPs samples; the ions would enhance the toxicity. Also, the total surface area in all samples was constant and so, the same amounts of Ag^+ were released. Thus, the toxicity was due to ions and the surface area played a key role.

Furthermore, it was observed that when the bacterial density (turbidity) is decreasing, the diameter of the inhibition zones is increased. This means that when less bacteria are spread on the agar plates, the bactericidal effect is stronger.

As mentioned before, the Kirby-Bauer method relies on the diffusivity of the tested compound in the agar. So, since the Ag^+ are those which diffuse, the toxic effect is due to Ag^+ release rate. So, the rate in which AgNPs dissolve and form Ag^+ is proportional to the total particle surface area. In all samples with AgNPs, regardless size and concentration, the inhibition zones had the same diameter.

A variation in the results was observed not only between the difference in the particle production method, but also in the difference in applying the bacteria and the filters. In the vaporization-condensation technique the inhibition zones are larger and their diameter increases as the size and the concentration increase. In addition this technique does not produce so pure NPs because of any impurities found in the furnace and the size distributions were broad. Also, these experiments lasted longer, so the particles had more time to interact with the atmospheric oxygen. So, maybe the formation of the Ag^+ had already started when the experiments were conducted. All these above may interfere to the observed results. With the AgNPs produced with the spark discharge technique, the inhibition zones were significantly smaller (AuNPs exhibited no inhibition zones), the particles were ultrapure and the size distributions were narrower.

When the NP-ladden filters (AgNPs since AuNPs did not form inhibition zone) were placed facing down and have direct interaction with the agar and the bacteria, inhibition zones were formed. When the NP-ladden filters were placed facing up, no direct interaction with the agar and the bacteria, and a small droplet of water was placed on top of them, again inhibition zone was formed. Also, when the NP-ladden filters were placed facing up and a small amount of bacterial suspension was placed on top of them, there was direct interaction with the bacteria but not with the agar. Bacterial growth was observed on top of them and the bacteria were intact, but these experiments should be investigated further with different sizes of NPs.

The calculations that follow are about the deposition time needed for each filter by keeping the surface area of a 30 nm particle constant.

First of all, we calculate the mass (M) of one particle:

$$M = V * \rho \tag{7}$$

With:

V: volume of one particle 30 nm (m³)

ρ: Ag or Au density (g/m³)

Then, the particles per surface area are calculated:

$$P = M * C \tag{8}$$

With:

C: the wanted concentration (g/m²)

Afterwards, the particles that will be deposited on the filter are calculated:

$$Pa = P * f \tag{9}$$

With:

f: the filter's surface area (m²)

The total surface area is calculated:

$$Tsa = Pa * psa \tag{10}$$

With:

psa: the surface area of one particle 30 nm (m²)

The particles that are produced at the spark chamber every minute are calculated:

$$Ps = Cm * Q \tag{11}$$

With:

Cm: the concentration measured from the CPC (#/m³)

Q: the flow that carries away the particles from the spark chamber (m³/min)

The particles for a specific surface area are calculated:

$$Psu = Tsa/psa \tag{12}$$

And so, the time needed for the acquired deposition on the filter:

$$t = Psu/Pa \tag{13}$$

References

Asghari, S., et al., (2012), 'Toxicity of various silver nanoparticles compared to silver ions in *Daphnia magna*', *Journal of Nanobiotechnology*, 10(14), pp. 1-11

Bae, E., et al., (2010), 'Bacterial Cytotoxicity of the Silver Nanoparticle related to Physicochemical metrics and Agglomeration properties', *Environmental Toxicology and Chemistry*, 29(10), pp. 2154-2160

Bae, E., et al., (2011), 'Effect of Chemical Stabilizers in Silver Nanoparticle Suspensions on Nanotoxicity', *Bulletin of the Korean Chemical Society*, 32(2), pp. 613-619

Bauer, A.W., et al., (1966), 'Antibiotic Susceptibility Testing by a Standardized Single Disk Method', *American Journal of Clinical Pathology*, 45, pp. 493-496

Buzea, C., Pacheco Blandino, I.I., Robbie, K. (2007), 'Nanomaterials and nanoparticles: Sources and toxicity', *Biointerphases,* 2(4), pp.MR17-MR172

Choi, O., et al., (2008), 'The inhibitory effects of silver nanoparticles, silver ions and silver chloride colloids on microbial growth', *Water Research*, 42, pp. 3066-3074

Cho, K.H., et al., (2005), 'The study of antimicrobial activity and preservative effects of nanosilver ingredient', *Electrochemica Acta*, 51, pp. 956-960

Chudasama, B., et al., (2010), 'Highly bacterial resistant silver nanoparticles: synthesis and antibacterial activities', *Journal of Nanoparticle Research*, 12, pp.1677-1685

Connor, E., et al., (2005), 'Gold Nanoparticles Are Taken Up by Human Cells but Do Not Cause Acute Cytotoxicity', *Small*, 1(3), pp. 325-327

Cui, Y., et al., (2012), 'The molecular mechanism of action of bactericidal gold nanoparticles on *Escherichia coli*', *Biomaterials*, 33, pp. 2327-2333

Devi, J.S. and Bhimba, B.V., (2012), 'Silver nanoparticles: Antibacterial activity against wound isolates & *in vitro* cytotoxic activity on Human Caucasian colon adenocarcinoma', *Asian Pacific Journal of Tropical Diseases*, pp. 87-93

Elsome, A., et al., (1996), 'Antimicrobial activities *in vitro* and *in vivo* of transition element complexes containing gold(I) and osmium(VI)', *Journal of Antimicrobial Chemotherapy*, 37, pp. 911-918

Espinosa-Cristóbal, L.F., et al., (2009), 'Antibacterial effect of silver nanoparticles against *Streptococcus mutans*', *Materials Letters*, 69, pp. 2603-0206

Fabrega, J., et al., (2009), 'Silver Nanoparticle Impact on Bacterial Growth: Effect of pH, Concentration, and Organic Matter', *Environmental Science & Technology*, 43(19), pp. 7285-7290

Fan, C., et al., (2011), 'Development of an antimicrobial resin-A pilot study', *Dental Materials*, 27, pp. 322-328

Feng, Q.L., et al., (2000), 'A mechanistic study of the antibacterial effect of silver ions on *Escherichia coli* and *Staphylococcus aureus*', *Journal of Biomedical Materials Research*, 52(4), pp. 662-668

Freitas, R. (2005), 'Current Status of Nanomedicine and Medical Nanorobotics'*, Journal of Computational and Theoretical Nanoscience*, 2, pp.1-25

Fricker, S.P. (1996), 'Medical Uses of Gold Compounds: Past, Present and Future', *Gold Bulletin*, 29(2), pp. 53-60

Geethalakshmi, R. and Sarada, D.V.L., (2012), 'Gold and silver nanoparticles from *Trianthema decandra*: synthesis, characterization, and antimicrobial properties', *International Journal of Nanomedicine*, 7, pp.5375-5384

Giamarelou, M. et al., (2012), 'The multiple monodisperse outlet differential mobility analyzer: derivation of its transfer function and resolution', *Aerosol Science and Technology*, 46, pp.951-965

Gopinath, V., et al., (2012), 'Biosynthesis of silver nanoparticles from *Tribulus terrestris* and its antimicrobial activity: A novel approach', *Colloids and Surfaces B: Biointerfaces*, 96, pp. 69-74

Guzman, M., et al., (2012), 'Synthesis and antibacterial activity of silver nanoparticles against gram-positive and gram-negative bacteria', *Nanomedicine: Nanotechnology, Biology, and Medicine*, 8, pp. 37-45

Hernández-Sierra, J.F., et al., (2008), 'The antimicrobial sensitivity of *Streptococcus mutans* to nanoparticles of silver, zinc oxide and gold', *Nanomedicine: Nanotechnology, Biology, and Medicine*, 4, pp. 237-240

Humphrey, J.H. and Lightbown, J.W., (1952), 'A general theory for plate assay of antibiotics with some practical applications', *National Institute for Medical Research*, pp. 129-143

Kaviya, S., et al., (2011), 'Green synthesis of silver nanoparticles using *Polyalthia longifolia* leaf extract along with D-Sorbitol: study of antibacterial activity', *Journal of Nanotechnology*, 2011, pp. 1-5

Khan, S., et al., (2011), 'Silver nanoparticles tolerant bacteria from sewage environment', *Journal of Environmental Sciences*, 23(2), pp. 346-352

Kim, J.S., et al., (2007), 'Antimicrobial effects of silver nanoparticles', *Nanomedicine: Nanotechnology, Biology, and Medicine*, 3, pp. 95-101

Kim, S.W., et al., (2011), 'Assay-dependent effect of silver nanoparticles to *Escherichia coli* and *Bacillus subtilis*', *Applied Microbiology and Biotechnology*, 92, pp. 1045-1052

Knutson, E.O., and Whitby, K.T., (1975), '*Acurate measurements of aerosol electric mobility moments*', *Journal of Aerosol Science*, 6 (6), pp. 453-460

Knutson, E.O., and Whitby, K.T., (1975), '*Aerosol classification by electric mobility: apparatus, theory and applications*', *Journal of Aerosol Science*, 6 (6), pp. 443-451

Lehtinen, K.E.J., et al., (2004), 'Three-body collisions as a particle formation mechanism in silver nanoparticles synthesis', Journal of Colloid and Interface Science, 274, pp. 526-530

Li, W.R., et al., (2010), 'Antibacterial activity and mechanism of silver nanoparticles on *Escherichia coli*', *Applied Microbial and Cell Physiology*, 85, pp. 1115-1122

Lok, C., et al., (2007), 'Silver nanoparticles: partial oxidation and antibacterial activities', *Journal of Biological Inorganic Chemistry*, 12, pp. 527-534

Morones, J.R., et al., (2005), 'The bactericidal effect of silver nanoparticles', *Nanotechnology*, 16, pp. 2346-2353

Nanda, A., and Saravanan, M., (2009), 'Biosynthesis of silver nanoparticles from Staphylococcus aureus and its antimicrobial activity against MRSA and MRSE', *Nanomedicine: Nanotechnology, Biology, and Medicine*, 5, pp. 452-456

Navarro, E., et al., (2008), 'Toxicity of Silver Nanoparticles to *Chlamydomonas reinhardtii*', *Environmental Science & Technology*, 42, pp. 8959-8964

Pal, S., Tak, Y.K., Song, J.M. (2007), 'Does the Antibacterial Activity of Silver Nanoparticles Depend on the Shape of the Nanoparticle? A Study of the Gram-Negative Bacterium *Escherichia coli*', *Applied and Environmental Microbiology*, 73(6), pp. 1712-1720

Pan, Y., et al., (2007), 'Size-Dependent Cytotoxicity of Gold Nanoparticles', *Small*, 3(11), pp. 1941-1949

Radzig, M.A., et al., (2013), 'Antibacterial effects of silver nanoparticles on gram-negative bacteria: Influence on the growth and biofilms formation, mechanisms of action', *Colloids and Surfaces B: Biointerfaces*, 102, pp. 300-306

Rattanaruengsrikul, V., et al. (2011), '*In Vitro* Efficacy and Toxicology Evaluation of Silver Nanoparticle-Loaded Gelatin Hydrogel Pads as Antibacterial Wound Dressings', *Journal of Applied Polymer Science*, 124, pp. 1668-1682

Shahverdi, A., et al., (2007), 'Synthesis and effect of silver nanoparticles on the antibacterial activity of different antibiotics against *Staphylococcus aureus* and *Escherichia coli*', *Nanomedicine: Nanotechnology, Biology, and Medicine*, 3, pp. 168-171

Simon-Deckers, A., et al., (2008), 'Impact of gold nanoparticles combined to X-Ray irradiation on bacteria', *Gold Bulletin*, 41(2), pp. 187-194

Sondi, I., Salopek-Sondi, B. (2004), 'Silver nanoparticles as antimicrobial agent: a case study on *E.coli* as a model for Gram-negative bacteria', *Journal of Colloid and Interface Science*, 275, pp. 177-182

Sotiriou, G.A., Pratsinis, S.E. (2010), 'Antibacterial Activity of Nanosilver Ions and Particles', *Environmental Science and Technology*, 44(14), pp. 5649-5654

Stolzenburg, M.R., and McMurry, P.H., (1991), 'An ultrafine aerosol condensation nucleus counter', *Aerosol Science and Technology*, 14, pp.48-65

Tabrizi, N.S., et al., (2009), 'Generation of nanoparticles by spark discharge', *Journal of Nanoparticle Research*, 11, pp. 315-332

Wang, S., et al. (2008), 'Challenge in understanding size and shape dependent toxicity of gold nanomaterials in human skin keratinocytes', *Chemical Physics Letters*, 463, pp. 145-149

Wegner, K., et al., (2011), 'Pilot plants for industrial nanoparticle production by flame spray pyrolisis', *KONA Powder and Particle Journal,* 29, pp. 251-265

Wijnhoven, S.W.P., (2009), 'Nano-silver – a review of available data and knowledge gaps in human and environmental risk assessment', *Nanotoxicology*, pp. 1-30

Xiu, Z., et al., (2012), 'Negligible Particle-Specific Antibacterial Activity of Silver Nanoparticles', *Nano Letters*, 12, pp. 4271-4275

Yamanaka, M., et al., (2005), 'Bactericidal Actions of a Silver Ion Solution on *Escherichia coli*, Studied by the Energy-Filtering Transmission Electron Microscopy and Proteomic Analysis', *Applied and Environmental Microbiology*, 71(11), pp. 7589-7593

Yen, H.J., Hsu, S., Tsai, C.L. (2009), 'Cytotoxicity and Immunological Response of Gold and Silver Nanoparticles of Different Sizes', *Small*, 5(13), pp. 1553-1561

Zhao, G., and Stevens, E., (1998), 'Multiple parameters for the comprehensive evaluation of the susceptibility of *Escherichia coli* to the silver ion', *BioMetals*, 11, pp. 27-32

Books

Goldstein, J., Newbury, D.E., Joy, D.C., Lyman, C.E., Echlin, P., Llfshin, E., Sawyer, L., and Michael, J.R. (2003), *'Scanning Electron Microscopy and X-ray Microanalysis'*, Springer, Third edition

Hinds, W.C. (1999), '*Aerosol Technology: properties, behavior and measurement of airborne particles*', Canada, Second edition

Mansoori, A. (2005), *'Principles of Nanotechnology: Molecular-based Study of Condensed Matter in Small Systems'*, USA: World Scientific

NSTC, *'National Nanotechnology Initiative: Leading to the Next Industrial Revolution'* A Report by the Interagency Working Group on Nanoscience", Engineering and Technology Committee on Technology, National Science and Technology Council, Washington, D.C. February (2000)

Dissertations and Theses

Afonso, R.V., 2007. *Production of nanoparticles and carbon nanotubes*. Erasmus Project. Technical University of Delft.

Kavarnoy, P., 2011. *Cytotoxicity analysis of silver nanoparticles against Escherichia coli, Streptococcus mutas and Staphylococcus aureus*. Master thesis. University of the Aegean.

Steiner, M.G., 2011. *High resolution mobility spectrometry of molecular ions and their effect on the charging probabilities of airborne particles under bipolar diffusion charging conditions*. Ph.D. University of Vienna.

Websites

Centers for Disease Control and Infection, (n.d.), *General Information*, (Last update: 3rd August 2012), http://www.cdc.gov/ecoli/general/index.html, (last visit 17th January 2013)

CPS Instruments Europe, (n.d.), *Comparison of Particle Sizing Methods*, http://www.cpsinstruments.eu/pdf/Compare%20Sizing%20Methods.pdf (last visit 16th April 2013)

Massachusetts Institute of Technology, (n.d.), Faculty of Chemistry, Area of Research Nanoscience, http://www.mit.edu/~chemistry/faculty/nanoscience.html (last visit 21st June 2012)

Medical Microbiology, Murray PR et al., (2002), *Bacterial Morphology*, http://micro.digitalproteus.com/morphology2.php, (last visit 17th January 2013)

National Institute of Allergy and Infectious Diseases, (n.d.), *Antimicrobial (Drug) Resistance*, (Last update: 30th April 2012), http://www.niaid.nih.gov/topics/antimicrobialresistance/examples/gramnegative/Pages/default.aspx, (last visit 17th January 2013)

University of Wisconsin, (2002-2013), *E.coli Genome Project*, http://www.genome.wisc.edu/resources/strains.htm, (last visit 31st May 2013)

Zyvex, Ralph Merkle, (n.d.), "*Feynman's Talk*", http://www.zyvex.com/nanotech/feynman.html (last visit 20th June 2012)